ESD-TR-90-031

Technical Report
883

Analysis of DMSK Demodulators for DMSK and DPSK Reception

B.F. McGuffin

16 July 1990

Lincoln Laboratory

MASSACHUSETTS INSTITUTE OF TECHNOLOGY

LEXINGTON, MASSACHUSETTS

Prepared for the Department of the Air Force under Contract F19628-90-C-0002.

This report is based on studies performed at Lincoln Laboratory, a center for research operated by Massachusetts Institute of Technology. The work was sponsored by the Department of the Air Force under Contract F19628-90-C-0002.

The ESD Public Affairs Office has reviewed this report, and it is releasable to the National Technical Information Service, where it will be available to the general public, including foreign nationals.

This technical report has been reviewed and is approved for publication.

FOR THE COMMANDER

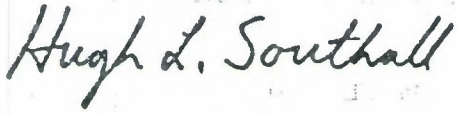

Hugh L. Southall, Lt. Col., USAF
Chief, ESD Lincoln Laboratory Project Office

Non-Lincoln Recipients

PLEASE DO NOT RETURN

Permission is given to destroy this document when it is no longer needed.

MASSACHUSETTS INSTITUTE OF TECHNOLOGY
LINCOLN LABORATORY

ANALYSIS OF DMSK DEMODULATORS FOR DMSK AND DPSK RECEPTION

B.F. McGUFFIN
Group 64

TECHNICAL REPORT 883

16 JULY 1990

LEXINGTON MASSACHUSETTS

ABSTRACT

This report considers some issues involved in using high data rate differential minimum shift keyed (DMSK) modulation to augment an existing satellite communication system employing differential phase shift keyed (DPSK) modulation. DMSK is preferred over DPSK for its greater spectral efficiency and robustness in nonlinear channels.

Two DMSK structures are discussed, the one- and two-bit demodulators, the second of which demodulates two interleaved differential data sequences. Analytic expressions are derived giving the bit error rate performance of both types of demodulator, with either matched or Gaussian filters. It is shown that the two-bit demodulator with a Gaussian filter provides the best performance in additive white Gaussian noise.

The use of a DMSK demodulator to receive DPSK signals is examined. This is of interest in order to reduce the number of demodulators required, while supporting augmented and original service. It is shown that the two-bit DMSK demodulator can be used to receive DPSK signals, but the one-bit demodulator cannot. Performance with filters that provide optimized DMSK demodulation and filters modified for DPSK signals are discussed. For a very small loss in DMSK performance, performance with DPSK signals can be brought to within 2 dB of the ideal DPSK demodulator.

TABLE OF CONTENTS

LIST OF ILLUSTRATIONS

LIST OF TABLES

1. INTRODUCTION

Differential minimum shift keyed (DMSK) signals and demodulators compare favorably with the more commonly used differential phase shift keyed (DPSK) signals for high data rate satellite communications [1,2,3]. DMSK signal spectra fall off more rapidly, allowing closer channel packing. Because DMSK signals have a constant envelope without requiring instantaneous carrier phase shifts, they suffer less distortion in nonlinear channels. Also, filtered DMSK does not suffer from sidelobe regrowth in nonlinear amplifiers. These advantages are obtained without greatly increasing complexity of on-board processing equipment. On the other hand, DPSK requires less power to achieve a specified bit error rate (BER) and has been used in existing systems.

As required data rates increase, DMSK becomes more attractive to communications satellite designers for its greater spectral efficiency. Increasing demand for high data rate services and resulting demands on the available spectrum continually increase the importance of using bandwidth-efficient modulation. This is true even for satellite channels, where design is usually driven by power constraints and where relatively abundant bandwidth has allowed spectral efficiency to be sacrificed for greater power efficiency. The appeal of DMSK is that it offers required spectral efficiency at a relatively low cost in power, and unlike many spectrally efficient modulation methods, DMSK is actually less sensitive to nonlinear channels than DPSK.

When implementing new satellite communications services to augment an existing system of satellites and ground terminals, it is highly desirable to remain backward compatible with existing services, so that current users may continue to function without replacing presently deployed equipment. The desire for backward compatibility and the relative simplicity of DPSK demodulators discourage the use of more bandwidth-efficient modulation schemes when augmenting existing services. The most direct approach to maintaining compatibility is to provide separate demodulators on board satellites for existing and new users. This increases satellite complexity and reduces channel assignment flexibility, thereby increasing weight and reducing channel utilization, as well as reducing satellite reliability.

In this report, a second option is examined for maintaining current services and providing new high data rate channels using bandwidth efficient modulation: the use of DMSK demodulators to receive DPSK signals. The goal is to provide relatively simple DMSK demodulators that can also support low rate DPSK users at a quality comparable to existing DPSK service. The use of DMSK demodulators to receive DPSK signals will be referred to as "DPSK cross support."

It will be shown that a correctly designed DMSK demodulator is capable of receiving DPSK signals operating at one-half the DMSK channel bit rate for which the demodulator was designed. Since multiple channel rate systems often use factor-of-two increments between supported channel rates, and the advantages of DMSK are more significant at higher channel bit rates, this data rate relation is convenient. If the demodulator design used requires a bank of analog detection filters to accommodate different channel data rates, this arrangement may actually reduce the number of required filters compared to an all-DPSK system. Actual savings in weight and complexity depend

on the ranges of channel data rates supported by existing and new modulation methods; however, if there is much overlap this savings can be considerable.

Using DPSK cross support will reduce the power efficiency of DPSK channels. It is shown here that DPSK cross support via DMSK demodulators incurs a signal-to-noise ratio (SNR) penalty of 2 to 4 dB relative to DPSK demodulators, depending on required channel BER and demodulator design. For a small penalty in DMSK performance ($\approx$0.1 dB), the cross support penalty can be reduced to 1.5 to 2 dB on the BER range 0.05 to 10^{-5}.

Section 2 contains an analysis of issues in DMSK demodulator design that are related to DMSK and DPSK cross support performance. DMSK signals are defined, and one- and two-bit differential coding is introduced. One-bit signals code information as the change in phase from one channel symbol to the next, while two-bit signals code information as the relative phase of two symbols on the same carrier component (in-phase or quadrature) which are separated in time by an intervening symbol on the opposing carrier component. Because DMSK demodulators suffer from relatively severe intersymbol interference (ISI), the choice of one- or two-bit demodulators has an impact on demodulator performance. Analytical expressions are introduced that give demodulator BER performance in terms of Marcum's generalized Q-function, assuming that detection filters are either matched to the MSK symbol, or are narrowband Gaussian filters with bandwidth to be specified by the designer. Using these expressions, it is seen that Gaussian filters provide superior performance for DMSK reception (up to several decibels), and that the most efficient system uses two-bit differential coding and Gaussian detection filters with normalized bandwidth (BT) ranging from 0.7 to 1.2 as the required BER ranges from 0.1 to 10^{-5}.

Section 3 shows that DPSK cross support can be provided by demodulators for two-bit DMSK signals, taking every other output bit as the demodulated bit sequence. Because the DPSK signal is coded entirely on the in-phase carrier component, one-bit DMSK demodulators are not suitable for receiving DPSK signals. A closed form expression is presented that gives cross support BER results in terms of Marcum's Q-function, and the issue of filter selection is reexamined with DPSK cross support in mind. Using the Gaussian filter, with bandwidth optimized for DMSK reception, results in 2 to 4 dB of DPSK performance degradation on the BER range 0.01 to 10^{-5}, relative to a DPSK demodulator. Optimizing the Gaussian filter bandwidth for DPSK cross support results in BT $\approx$0.5 for all BERs. DPSK cross support performance with this filter is degraded by 0.6 to 0.9 dB, but DMSK performance is degraded by 4 dB. Choosing an intermediate value for BT to minimize total power, assuming a 50% duty cycle for each signal type, results in DPSK degradation of 1.5 to 2 dB relative to a DPSK demodulator, and DMSK degradation of $\approx$0.1 dB.

The Appendix contains supporting material for BER expressions used in Sections 2 and 3.

2. DMSK DEMODULATORS

2.1 MSK Signals

An MSK signal can be modeled as an offset QPSK signal with overlapping half-cosine pulses. In complex notation the signal is

$$e(t) = Re\left\{(u_M(t) + z(t))e^{j(\omega_c t+\theta)}\right\} \tag{2.1}$$

where:

$u_M(t)$ is the equivalent baseband MSK signal;

$z(t)$ is a complex, zero-mean Gaussian noise process;

ω_c is the carrier or IF center frequency;

θ is an unknown phase constant.

The MSK equivalent baseband signal, with data rate $1/T$ bits per second, is given by

$$u_M(t) = \sqrt{2P}\left[\sum_{k\ even} d_k \widetilde{\cos}\left(\frac{\pi(t-kT)}{2T}\right) - j\sum_{k\ odd} d_k \widetilde{\cos}\left(\frac{\pi(t-kT)}{2T}\right)\right] \tag{2.2}$$

where:

P is signal power;

d_k are channel bits, with value ± 1;

$\widetilde{\cos}(\pi t/2T)$ is the baseband MSK pulse, with duration 2T [1]:

$$\widetilde{cos}(x) = \begin{cases} \cos(x) & -\pi/2 \le x \le \pi/2 \\ 0 & elsewhere. \end{cases} \tag{2.3}$$

Alternate pulses are modulated onto the in-phase and quadrature carrier channels and overlap in time. With coherent demodulation it is possible to separate the two carrier channels in the demodulator, but using differential demodulators overlapping pulses will cause significant ISI in the decision variable.

For an additive white Gaussian noise (AWGN) channel with noise power spectrum density (PSD) $N_0/2$, z(t) has autocorrelation function

$$\frac{1}{2}E\{z^*(t)z(t-\tau)\} = N_0\delta(\tau). \tag{2.4}$$

Demodulator structures for differential detection of MSK signals are discussed below.

2.2 DMSK Demodulator Structures

Two DMSK demodulator structures, the one- and two-bit demodulators [4 and references therein] are considered here. "One- and two-bit" refers to the length of delay used (in channel bit periods) on the delayed signal path in a delay and multiply differential demodulator.

Figure 2-1 illustrates the one-bit demodulator, for which consecutive bits are differentially encoded. This DMSK demodulator appears most often in the literature. Figure 2-1(a) is an IF implementation, and Figure 2-1(b) is a baseband version of the same demodulator (double lines identify complex signals). In the IF version of the one-bit demodulator, the signal is bandpass filtered, then multiplied by a delayed, phase-shifted version of itself. The delayed signal lags behind the current signal by T sec. Phase shifting is shown in two steps: the delayed signal is first multiplied by j, then complex-conjugated. This procedure translates the signal to baseband and removes unknown phase, except for a factor of $e^{j\omega_c T}$. The product is multiplied by $e^{-j\omega_c T}$ to remove the undesired phase term, which will be ignored in the remainder of this report. The real part of the baseband multiplier output is hard-limited to provide an estimate of $d_k d_{k-1}$. A factor of j is required in the delay branch because d_k and d_{k-1} are modulated in quadrature. The characteristic of the lowpass filter shown in the baseband demodulator is the equivalent baseband version of the bandpass filter used in the IF demodulator.

It has been observed several times [2,4,5] that DMSK demodulator performance may improve if differentially encoded symbols are separated by more than T sec. Such a signal can be constructed by interleaving n independent differentially encoded data sequences prior to modulation. Using these data sequences increases the required number of phase reference bits per frame from 1 to n. A minimum of 1 nT-sec delay is required in the demodulator to decode the channel bit sequence. Overall, there is little cost in complexity for using this differential code, and overhead costs are low if n is small relative to the frame size. Improved performance comes about from reduced noise correlation between samples and from changing the correlation between desired and ISI components of filtered signals entering the multiplier. For $n = 2$, one differentially encoded data sequence is modulated onto the in-phase carrier component, and a second is modulated onto the quadrature carrier component. It is shown in [5] that longer delays produce little additional improvement in demodulator performance, and only the $n = 2$ case will be considered here. The $n = 2$ receiver is called the two-bit demodulator.

Structures for the two-bit demodulator are shown in Figures 2-2(a) and 2-2(b) for IF and baseband implementation, respectively. This DMSK demodulator differs from the one-bit demodulator in that delayed versions of the filtered signal are delayed for $2T$ sec and are conjugated, but not multiplied by j. The demodulator output sequence estimates values of $d_k d_{k-2}$. The two-bit demodulator decision variable has an asymmetric constellation and, consequently, optimal detection requires comparing the real part of the multiplier output with a nonzero threshold. However, if the transmitted MSK signal is not subjected to narrowband filtering ($B < 1/2T$) in the transmitter or channel, then performance degradation is negligible for the Gaussian-filtered demodulator [3,4]. In order to avoid using fine automatic gain controls (AGCs) in the receiver, zero thresholds will be used in two-bit demodulators.

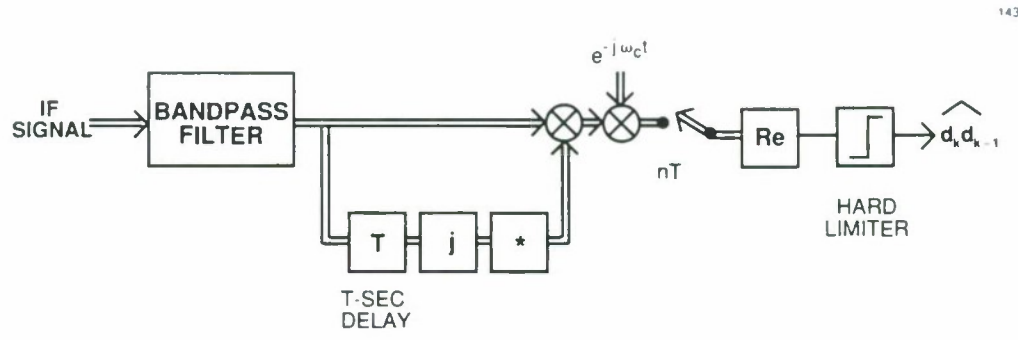

(a) IF DEMODULATOR

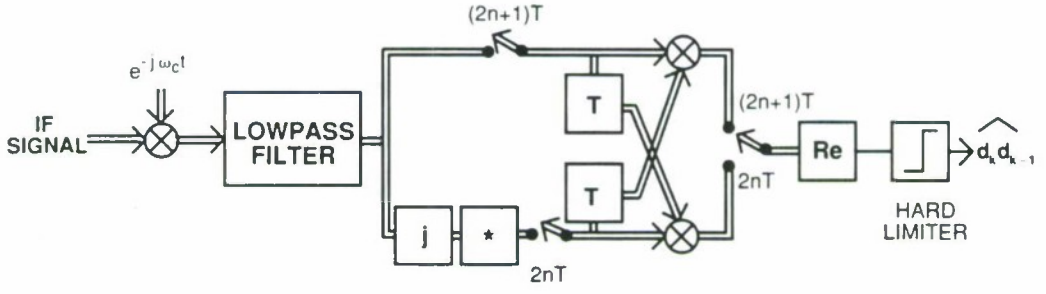

(b) BASEBAND DEMODULATOR

Figure 2-1. One-bit DMSK demodulator structures.

Complexity of the two demodulators is nearly identical, using the structures shown. The bandpass or lowpass detection filters must satisfy the same requirements for either demodulator. The two-bit demodulator does require one more delay element than the one-bit. Two-bit performance could be improved somewhat by adding a fine AGC and nonzero detection threshold, but that configuration will not be considered in this report.

Matched and Gaussian filters will be considered next for the demodulator bandpass or lowpass detection filters shown in Figures 2-1 and 2-2.

2.3 Matched Filters

One possible choice for detection filters in DMSK receivers is filters matched to the DMSK signal pulse. This is the optimal filter for coherent MSK demodulation, and matched filters are

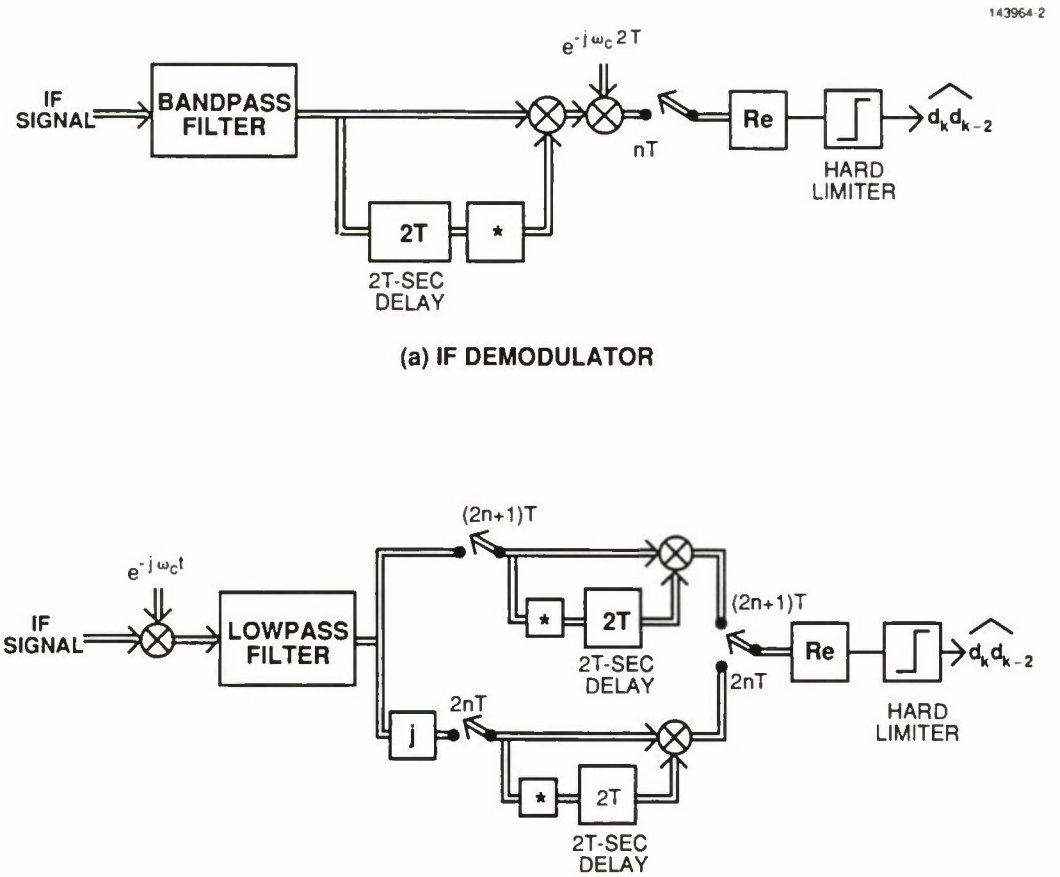

Figure 2-2. Two-bit DMSK demodulator structures.

known to provide good performance in DPSK receivers.

The matched filter for MSK signals has equivalent baseband impulse response

$$h_M(t) = \widetilde{\cos}\left(\frac{\pi t}{2T}\right). \tag{2.5}$$

This filter impulse response is unrealizable, but it has finite duration and can be realized as defined with the addition of a T-sec delay. Using $h_M(t)$ as defined, the equivalent baseband matched-filtered symbol pulse is given by

$$S_M(t) = \int_{-\infty}^{\infty} \widetilde{\cos}\left(\frac{\pi\tau}{2T}\right) \widetilde{\cos}\left(\frac{\pi(t-\tau)}{2T}\right) d\tau, \tag{2.6}$$

and the filtered baseband equivalent signal is

$$v_M(t) = \sqrt{2P}\left[\sum_{k\ even} d_k\, S_M(t-kT) - j\sum_{k\ odd} d_k\, S_M(t-kT)\right] + n_M(t) \tag{2.7}$$

where $n_M(t)$ is the equivalent baseband matched-filtered noise process.

$S_M(t)$ can be written as the integral of a product of cosines, with the limits of integration appropriately modified to reflect the finite extent of $\widetilde{\cos}(\pi t/2T)$. The limits of integration depend on whether t is greater or less than zero. Both cases combine to give the final form of $S_M(t)$ as

$$S_M(t) = \begin{cases} T\cos\left(\frac{\pi t}{2T}\right)\left(1-\frac{|t|}{2T}\right) + \frac{T}{\pi}\sin\left(\frac{\pi|t|}{2T}\right) & -2T < t < 2T \\ 0 & elsewhere. \end{cases} \tag{2.8}$$

$S_M(t)/T$ is plotted in Figure 2-3. Some important values of the matched-filtered symbol pulse are

$$\begin{aligned} S_M(0) &= T \\ S_M(\pm T) &= T/\pi \\ S_M(\pm nT) &= 0 \quad n = 2,\ 3,\ 4, \ldots \end{aligned}$$

The last relation indicates that each pulse will experience ISI only from the immediately preceding and following pulses.

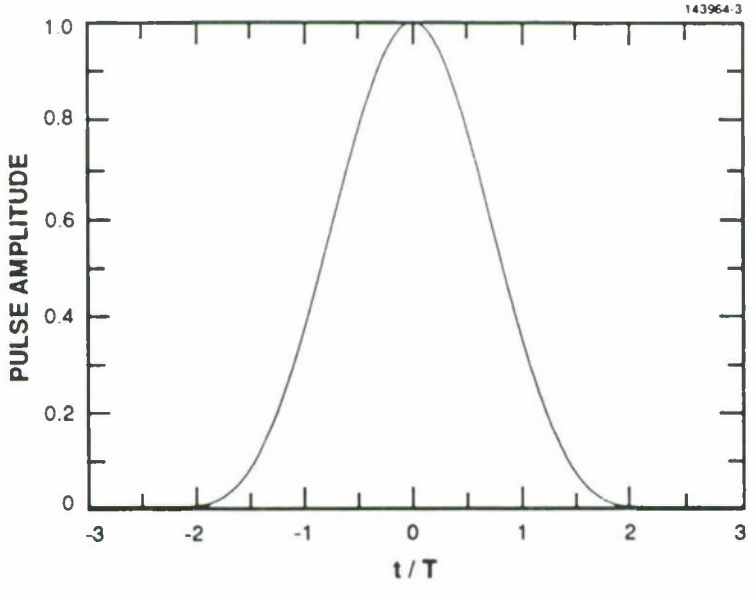

Figure 2-3. MSK matched-filtered symbol pulse.

The equivalent baseband matched-filtered noise process is

$$n_M(t) = \int_{-\infty}^{\infty} z(t-\tau)\widetilde{\cos}\left(\frac{\pi\tau}{2T}\right) d\tau. \tag{2.9}$$

The filtered noise autocorrelation function is found using Equation (2.4) to be

$$R_M(\tau) \equiv \frac{1}{2}\mathrm{E}\{n_M^*(t-\tau)n_M(t)\} = N_0 \int_{-\infty}^{\infty} \widetilde{\cos}\left(\frac{\pi u}{2T}\right) \widetilde{\cos}\left(\frac{\pi(\tau-u)}{2T}\right) du \tag{2.10}$$

which is

$$R_M(\tau) = N_0 S_M(\tau). \tag{2.11}$$

Note that noise samples are uncorrelated if they are taken $2T$ or more seconds apart.

2.4 Gaussian Filters

Another possible choice for DMSK detection filters is the Gaussian filter. This has a perfectly linear phase response and is frequently used both for analyzing and constructing DMSK receivers. Numerous examples can be found in the bibliographies of [3,4,6].

A bandpass Gaussian filter has equivalent baseband impulse and frequency responses

$$h_G(t) = \frac{k_1 B}{\sqrt{\pi}} e^{-(k_1 B t)^2} \tag{2.12}$$

and

$$H_G(\omega) = e^{-(\omega/2k_1 B)^2}, \tag{2.13}$$

respectively. B is the bandpass filter half-power bandwidth (B is twice the lowpass filter half-power bandwidth) and $k_1 = \pi/\sqrt{2\log(2)} \approx 2.6682$.

Using the Gaussian filter, the equivalent baseband symbol pulse is

$$S_G(t) = \frac{k_1 B}{\sqrt{\pi}} \int_{-\infty}^{\infty} \widetilde{\cos}\left(\frac{\pi(t-\tau)}{2T}\right) e^{-(k_1 B\tau)^2} d\tau \tag{2.14}$$

and the equivalent baseband filtered signal is

$$v_G(t) = \sqrt{2P}\left[\sum_{k\ even} d_k\, S_G(t-kT) - j\sum_{k\ odd} d_k\, S_G(t-kT)\right] + n_G(t). \tag{2.15}$$

The integral for $S_G(t)$ is evaluated by substituting a pair of complex exponentials for $\widetilde{\cos}(\pi t/2T)$ in the region where it is nonzero, then completing the square in the exponents. The resulting integral can be expressed in terms of erfc($\cdot$), the complementary Gaussian error function, as

$$\begin{aligned} S_G(t) \;=\; & e^{-\left(\frac{\pi}{4k_1 BT}\right)^2} Re\left\{e^{j\pi t/2T}\left[\mathrm{erfc}\left(k_1 BT\left(1+\frac{t}{T}\right) + j\frac{\pi}{4k_1 BT}\right)\right.\right. \\ & \left.\left. -\mathrm{erfc}\left(-k_1 BT\left(1-\frac{t}{T}\right) + j\frac{\pi}{4k_1 BT}\right)\right]\right\}. \end{aligned} \tag{2.16}$$

Numerical approximations exist that can be used to find the value of erfc(·) with a complex argument [7]. Figure 2-4 shows the shape of $S(t)$ for several values of BT. It is apparent in Figure 2-4 that for BT ≥ 0.6, each data pulse will receive significant ISI only from the immediately preceding and following pulses. The filtered baseband noise process, $n_G(t)$, is

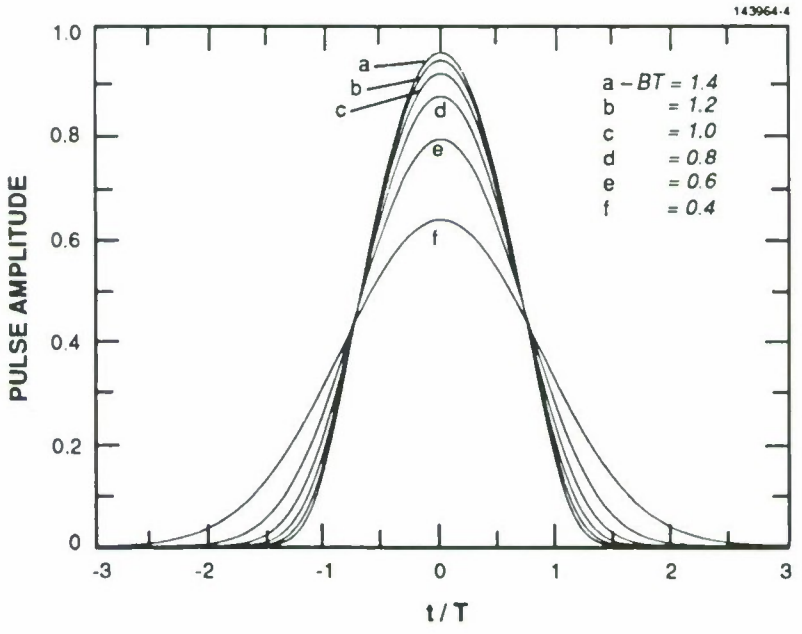

Figure 2-4. MSK Gaussian-filtered symbol pulse.

$$n_G(t) = \frac{k_1 B}{\sqrt{\pi}} \int_{-\infty}^{\infty} z(t-\tau) e^{-(k_1 B\tau)^2} d\tau. \tag{2.17}$$

Using Equation (2.4), the autocorrelation function of this integral can be evaluated as

$$R_G(\tau) \equiv \frac{1}{2} E\{n_G^*(t-\tau) n_G(t)\} = \frac{k_1 N_0 B}{\sqrt{2\pi}} e^{-(k_1 B\tau)^2/2}. \tag{2.18}$$

Noise autocorrelation falls off exponentially with the time separation between noise samples and can be considered negligible for $|\tau| \geq 2T$ if BT ≥ 0.6.

2.5 One-Bit Demodulator Performance

In order to determine the performance of the one-bit DMSK demodulator, consider the value of the equivalent baseband signal at time $t = kT$, for even k. Because the equivalent baseband-filtered

symbol pulse is very small for $|t| \geq 2T$ (zero for the matched filter), it can be assumed that only three data symbols affect the signal value:

$$v(kT) = \sqrt{2P}\,[d_k S(0) - j(d_{k-1} + d_{k+1})S(T)] + n(kT). \tag{2.19}$$

This signal is multiplied by a conjugated version of the signal value at time $t = (k-1)T$:

$$jv((k-1)T) = \sqrt{2P}\,[d_{k-1} S(0) + j(d_{k-2} + d_k)S(T)] + jn((k-1)T) \tag{2.20}$$

where the factor j in the delay branch has been absorbed into the signal sample. The resulting decision variable is

$$\begin{aligned} v(kT)[jv((k-1)T)]^* = 2P \Big\{ & S^2(0) d_k d_{k-1} \\ & - S^2(T)(d_{k-1} + d_{k+1})(d_{k-2} + d_k) \\ & - jS(0)S(T)[d_{k-1}(d_{k-1} + d_{k+1}) + d_k(d_{k-2} + d_k)]\Big\} \\ & + noise. \end{aligned} \tag{2.21}$$

The desired value of this variable is $2P d_k d_{k-1} S^2(0)$; other deterministic terms represent ISI. The decision variable constellation is shown in Figure 2-5, where each point represents the decision variable with a different ISI pattern. Points in the positive real half-plane represent the event that $d_k = d_{k-1}$, and points on the negative real half-plane represent the event $d_k \neq d_{k-1}$. Probabilities are assigned to the constellation points assuming that bit values are independent, and take the values ± 1 with equal probability. Table 2-1 lists the probability for each constellation point. Proceeding as above for odd k results in the same constellation and probabilities.

TABLE 2-1.

One-Bit DMSK Demodulator Constellation Probabilities

Correct Decision	Constellation Point	Data Values	Probability
$d_k = d_{k-1}$:	1	$d_{k-2} + d_k = d_{k-1} + d_{k+1} = 0$	1/8
	2	$d_{k-2} + d_k = d_{k-1} + d_{k+1} = \pm 2$	1/8
	3	$d_{k-2} + d_k = 0,\ d_{k-1} + d_{k+1} = \pm 2$	1/8
	3	$d_{k-2} + d_k = \pm 2,\ d_{k-1} + d_{k+1} = 0$	1/8
$d_k \neq d_{k-1}$:	4	$d_{k-2} + d_k = d_{k-1} + d_{k+1} = 0$	1/8
	5	$d_{k-2} + d_k = -(d_{k-1} + d_{k+1}) = \pm 2$	1/8
	6	$d_{k-2} + d_k = 0,\ d_{k-1} + d_{k+1} = \pm 2$	1/8
	6	$d_{k-2} + d_k = \pm 2,\ d_{k-1} + d_{k+1} = 0$	1/8

The demodulator estimates $d_k d_{k-1}$ by the sign of the real part of $v(kT)[jv((k-1)T)]^*$. The probability of error for a particular ISI pattern can be found using the methods of Stein [8,9] for

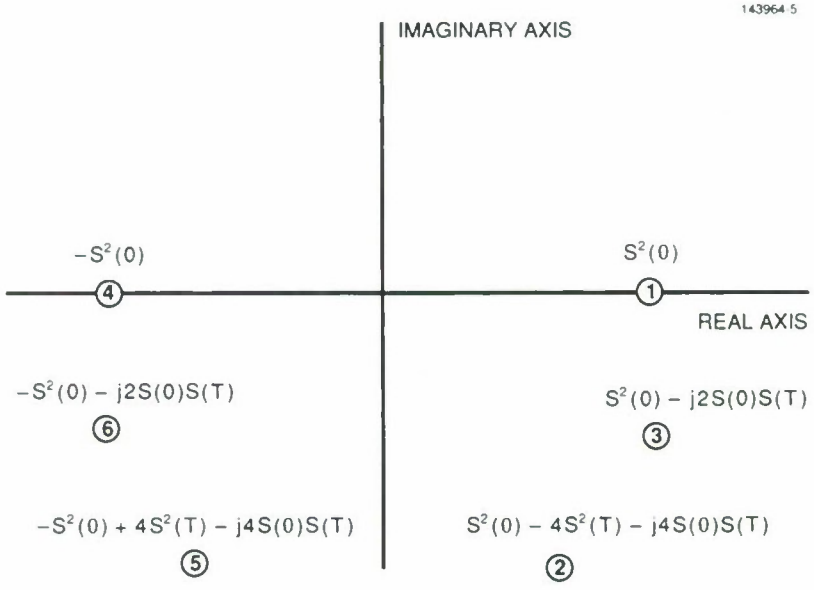

Figure 2-5. One-bit DMSK demodulator constellation.

binary DPSK detection. These conditional error probabilities are then averaged over ISI to produce the demodulator BER. Because the constellation is symmetric about the imaginary axis, only the case $d_k = d_{k-1}$ must be considered. This procedure is carried out in the Appendix.

For the matched-filtered one-bit DMSK demodulator the probability of error is

$$\begin{aligned} P_e &= \frac{1}{2} + \frac{3}{8} Q\left(\sqrt{\frac{E_B}{N_0} c\left(1 - \frac{1}{\sqrt{c}}\right)}, \sqrt{\frac{E_B}{N_0} c\left(1 + \frac{1}{\sqrt{c}}\right)}\right) \\ &- \frac{3}{8} Q\left(\sqrt{\frac{E_B}{N_0} c\left(1 + \frac{1}{\sqrt{c}}\right)}, \sqrt{\frac{E_B}{N_0} c\left(1 - \frac{1}{\sqrt{c}}\right)}\right) \\ &+ \frac{1}{8} Q\left(\sqrt{\frac{E_B}{N_0} c\left(1 - \frac{1 - 4/\pi^2}{\sqrt{c}}\right)}, \sqrt{\frac{E_B}{N_0} c\left(1 + \frac{1 - 4/\pi^2}{\sqrt{c}}\right)}\right) \\ &- \frac{1}{8} Q\left(\sqrt{\frac{E_B}{N_0} c\left(1 + \frac{1 - 4/\pi^2}{\sqrt{c}}\right)}, \sqrt{\frac{E_B}{N_0} c\left(1 - \frac{1 - 4/\pi^2}{\sqrt{c}}\right)}\right) \end{aligned} \tag{2.22}$$

where $c = \pi^2/(\pi^2 - 1)$, and $Q(\cdot, \cdot)$ is Marcum's Q-function. (Figure 2-6 graphs this expression.)

From the Appendix, BER for the Gaussian-filtered one-bit demodulator is

$$\begin{aligned} P_e &= \frac{1}{2} + \frac{1}{4}\left[Q(\sqrt{a_3}, \sqrt{b_3}) - Q(\sqrt{b_3}, \sqrt{a_3})\right] \\ &+ \frac{1}{8}\left[Q(\sqrt{a_1}, \sqrt{b_1}) - Q(\sqrt{b_1}, \sqrt{a_1})\right] \end{aligned}$$

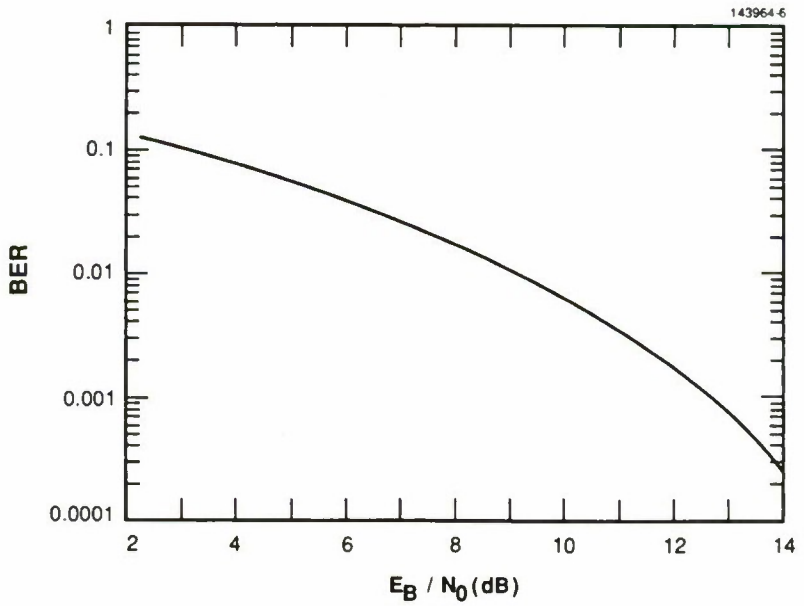

Figure 2-6. Matched-filtered one-bit DMSK demodulator performance.

$$+\frac{1}{8}\left[Q(\sqrt{a_2},\sqrt{b_2})-Q(\sqrt{b_2},\sqrt{a_2})\right] \tag{2.23}$$

where the coefficients for this expression are given by Equations (A.30), (A.33), and (A.38) of the Appendix.

Performance of the Gaussian-filtered demodulator is a function of filter bandwidth; BT appears explicitly in the definitions of a_i and b_i for $i = 1, 2, 3$, and through values of $S_G(t)$ appearing in those expressions. The optimal value of BT varies with desired BER. Figure 2-7 plots Equation (2.23) for several values of BT. The bottom curve was made by varying BT to minimize the BER at each value of E_B/N_0. Table 2-2 lists some points from the optimized curve in Figure 2-7.

TABLE 2-2.

Gaussian-Filtered One-Bit DMSK Demodulator Optimal BT

BER	Optimal BT	Required E_B/N_0 (dB)
10^{-1}	0.67	3.02
10^{-2}	0.85	7.74
10^{-3}	1.00	10.37
10^{-4}	1.09	12.15
10^{-5}	1.14	13.48

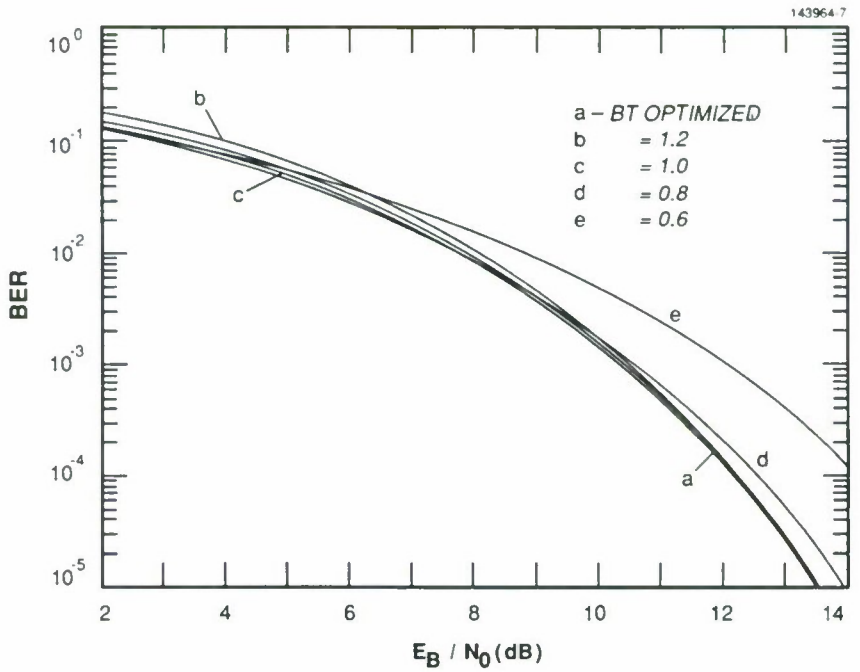

Figure 2-7. Gaussian-filtered one-bit DMSK demodulator performance.

An actual demodulator will operate with fixed BT, which will be suboptimal at most operating points. For desired BER in the range 0.08 to 0.006, performance with BT = 0.8 is very close to optimal.

2.6 Two-Bit Demodulator Performance

Assuming as before that $S(t) \approx 0$ for $|t| \geq 2T$, the value of $v(kT)$, the equivalent baseband signal at time $t = kT$ for even k, is given by Equation (2.19). The delayed signal is now

$$v((k-2)T) = \sqrt{2P}\,[d_{k-2}S(0) - j(d_{k-3} + d_{k-1})S(T)] + n((k-2)T) \tag{2.24}$$

and the resulting decision variable is

$$\begin{aligned} v(kT)v^*((k-2)T) = 2P\Big\{ & d_k d_{k-2} S^2(0) \\ & + S^2(T)(d_{k-1} + d_{k+1})(d_{k-3} + d_{k-1}) \\ & + jS(0)S(T)[d_k(d_{k-1} + d_{k-3}) - d_{k-2}(d_{k+1} + d_{k-1})]\Big\} \\ & + noise. \end{aligned} \tag{2.25}$$

The desired value of this variable is $2Pd_k d_{k-2} S^2(0)$, and other deterministic terms in the decision variable represent ISI. The decision variable constellation is shown in Figure 2-8. Each point of the

constellation represents a different ISI pattern. For convenience, some points that are reflections of each other across the real axis, which by symmetry will have the same conditional error rate, have been lumped together. Points in the positive real half-plane represent the event that $d_k = d_{k-2}$, and points on the negative real half-plane represent the event $d_k \neq d_{k-2}$. Probabilities are assigned to the constellation points assuming that bit values are independent and take the values ± 1 with equal probability. The probability of each constellation point occurring is listed in Table 2-3. Proceeding as above for odd k results in the same constellation and probability distribution.

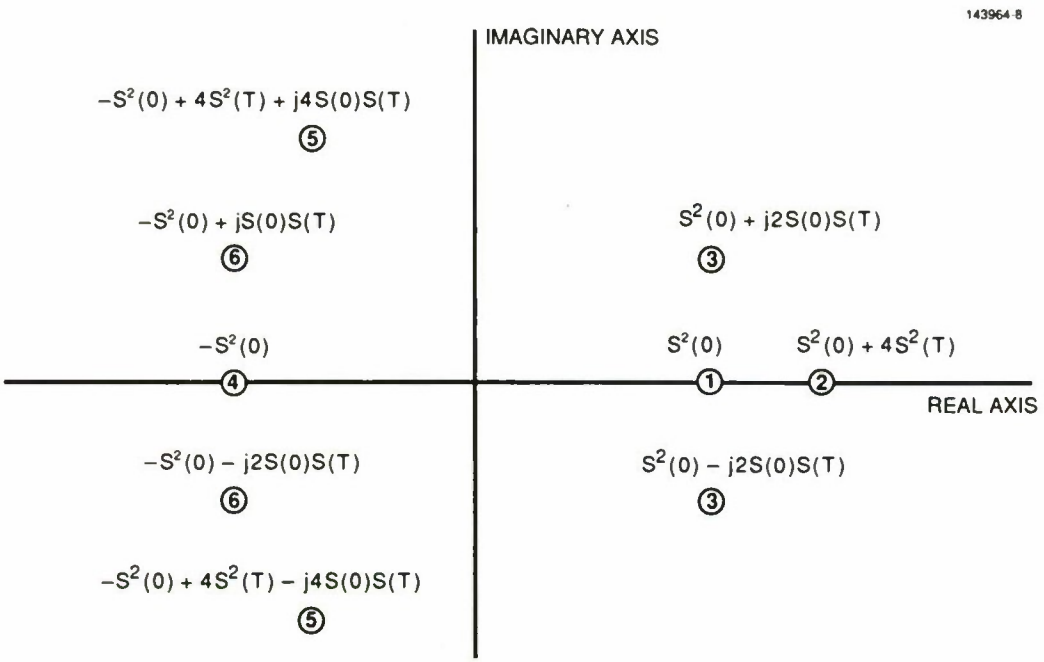

Figure 2-8. Two-bit DMSK demodulator constellation.

The demodulator estimates $d_k d_{k-2}$ by the sign of the real part of $v(kT)v^*((k-2)T)$. The BER can be found as it was for the one-bit demodulator, finding the conditional error probability for each possible ISI pattern, then averaging over ISI. As the constellation is not symmetric about the imaginary axis, BER must be found for $d_k = d_{k-2}$ and for $d_k \neq d_{k-2}$, and the two results averaged. Conditional error probabilities are found in the Appendix.

For the matched-filter two-bit DMSK demodulator, the probability of error is

$$\begin{aligned} P_e &= \frac{1}{16}\left[5 + e^{-E_B/N_0}\left(2 + e^{-4E_B/\pi^2 N_0}\right)\right] \\ &+ \frac{1}{4}Q\left(\sqrt{\frac{E_B}{N_0}\frac{2}{\pi^2}}, \sqrt{\frac{E_B}{N_0}\left(2 + \frac{2}{\pi^2}\right)}\right) \\ &- \frac{1}{4}Q\left(\sqrt{\frac{E_B}{N_0}\left(2 + \frac{2}{\pi^2}\right)}, \sqrt{\frac{E_B}{N_0}\frac{2}{\pi^2}}\right) \end{aligned}$$

TABLE 2-3.

Two-Bit DMSK Demodulator Constellation Probabilities

Correct Decision	Constellation Point	Data Values	Probability
$d_k = d_{k-2}$:	1	$d_{k-3} + d_{k-1} = d_{k-1} + d_{k+1} = 0$	1/8
	2	$d_{k-3} + d_{k-1} = d_{k-1} + d_{k+1} = \pm 2$	1/8
	3	$d_{k-3} + d_{k-1} = 0,\ d_{k-1} + d_{k+1} = \pm 2$	1/8
	3	$d_{k-3} + d_{k-1} = \pm 2,\ d_{k-1} + d_{k+1} = 0$	1/8
$d_k \neq d_{k-2}$:	4	$d_{k-3} + d_{k-1} = d_{k-1} + d_{k+1} = 0$	1/8
	5	$d_{k-3} + d_{k-1} = d_{k-1} + d_{k+1} = \pm 2$	1/8
	6	$d_{k-3} + d_{k-1} = 0,\ d_{k-1} + d_{k+1} = \pm 2$	1/8
	6	$d_{k-3} + d_{k-1} = \pm 2,\ d_{k-1} + d_{k+1} = 0$	1/8

$$+ \quad \frac{1}{16}\left[Q\left(\sqrt{\frac{E_B}{N_0}\frac{8}{\pi^2}}, \sqrt{\frac{E_B}{N_0}2}\right) - Q\left(\sqrt{\frac{E_C}{N_0}2}, \sqrt{\frac{E_B}{N_0}\frac{8}{\pi^2}}\right)\right]. \tag{2.26}$$

This expression is graphed in Figure 2-9.

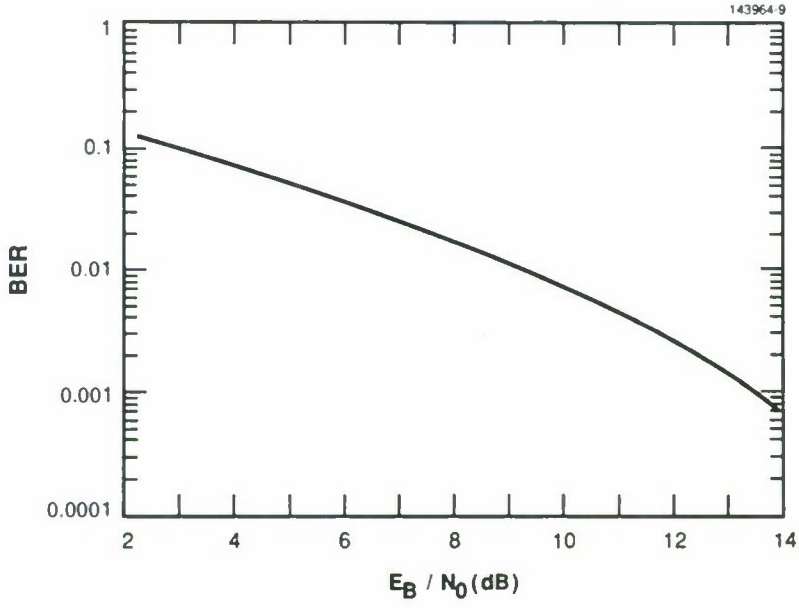

Figure 2-9. Matched-filtered two-bit DMSK demodulator performance.

From the Appendix, BER for the Gaussian-filtered two-bit demodulator is

$$P_e = \frac{1}{16}\left[5 + e^{-\frac{E_B}{N_0}\frac{2\sqrt{2\pi}}{k_1 BT}S_G^2(0)}\left(2 + e^{-\frac{E_B}{N_0}\frac{2\sqrt{2\pi}}{k_1 BT}4S_G^2(T)}\right)\right]$$

$$+ \quad \frac{1}{4}Q\left(\sqrt{\frac{E_B}{N_0}\frac{2\sqrt{2\pi}}{k_1BT}}S_G(T),\ \sqrt{\frac{E_B}{N_0}\frac{2\sqrt{2\pi}}{k_1BT}\left(S_G^2(0)+S_G^2(T)\right)}\right)$$

$$- \quad \frac{1}{4}Q\left(\sqrt{\frac{E_B}{N_0}\frac{2\sqrt{2\pi}}{k_1BT}\left(S_G^2(0)+S_G^2(T)\right)},\ \sqrt{\frac{E_B}{N_0}\frac{2\sqrt{2\pi}}{k_1BT}}S_G(T)\right)$$

$$+ \quad \frac{1}{16}Q\left(\sqrt{\frac{E_B}{N_0}\frac{2\sqrt{2\pi}}{k_1BT}}2S_G(T),\ \sqrt{\frac{E_B}{N_0}\frac{2\sqrt{2\pi}}{k_1BT}}S_G(0)\right)$$

$$- \quad \frac{1}{16}Q\left(\sqrt{\frac{E_B}{N_0}\frac{2\sqrt{2\pi}}{k_1BT}}S_G(0),\ \sqrt{\frac{E_B}{N_0}\frac{2\sqrt{2\pi}}{k_1BT}}2S_G(T)\right). \tag{2.27}$$

As before, performance of the Gaussian-filtered demodulator is a function of filter bandwidth. The optimal value of BT varies with desired BER. Figure 2-10 shows curves of P_e versus E_B/N_0 for several values of BT. The figure also includes a curve plotted using the optimal value of BT at each power level. Table 2-4 lists some of the points on the optimized curve in Figure 2-10.

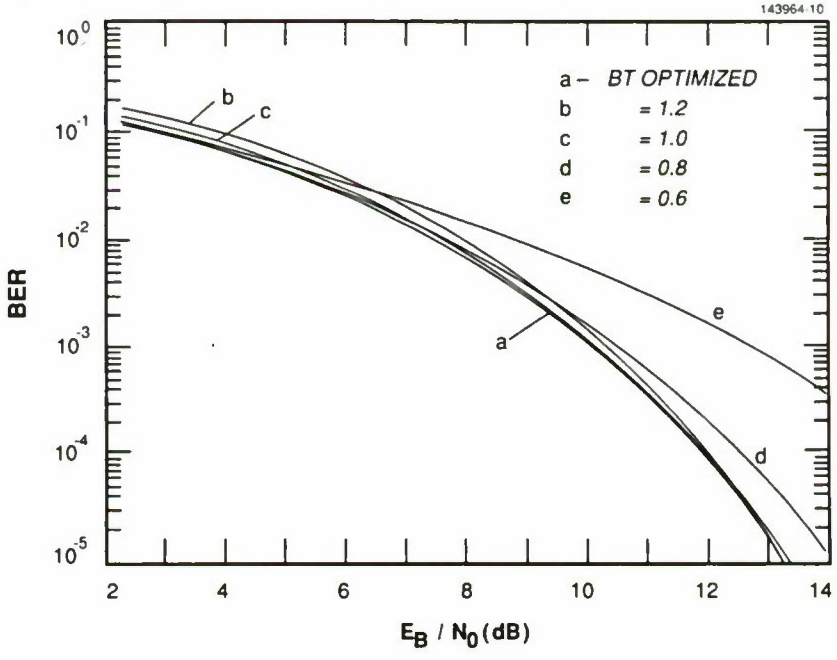

Figure 2-10. Gaussian-filtered two-bit DMSK demodulator performance.

An actual demodulator will operate with fixed BT, which will be suboptimal for most operating points. For desired BER in the range 0.1 to 0.006, BT = 0.8 produces results very close to the optimum.

TABLE 2-4.

Gaussian-Filtered Two-Bit DMSK Demodulator Optimal BT

BER	Optimal BT	Required E_B/N_0 (dB)
10^{-1}	0.69	2.81
10^{-2}	0.86	7.42
10^{-3}	1.00	10.01
10^{-4}	1.09	11.81
10^{-5}	1.16	13.18

2.7 Comparison of DMSK Demodulators

Figure 2-11 shows BER performance for all four DMSK demodulators that have been considered here, as a function of E_B/N_0. For Gaussian-filtered demodulators, the optimal filter bandwidth was used at each SNR.

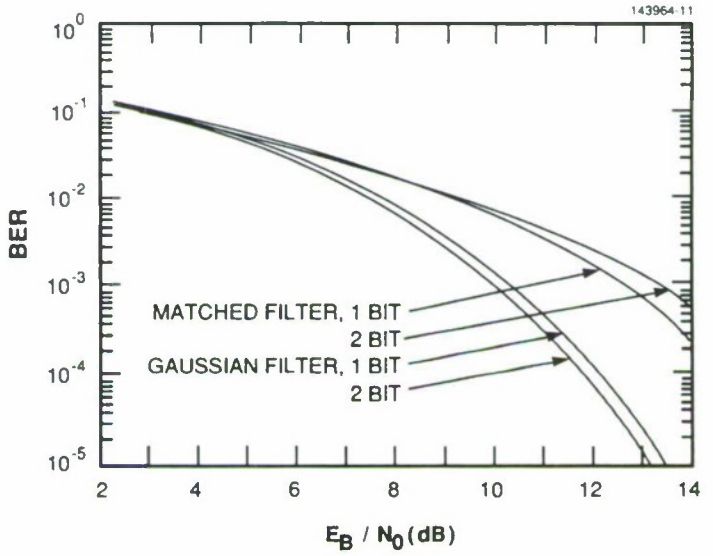

Figure 2-11. DMSK demodulator performance, matched and optimized Gaussian filters.

Gaussian detection filters provide superior performance to matched filters for either demodulator structure. For BER = 0.01, using matched filters costs ≈1.5 dB of SNR. The cost increases rapidly at lower BERs. It is interesting to note that the two-bit demodulator performs better than the one-bit when both are equipped with Gaussian detection filters, but with matched filters

performance of the two-bit demodulator is worse than that of the one-bit for BER <0.001. As E_B/N_0 grows, BER curves for one- and two-bit Gaussian demodulators grow closer together and may also cross at some high value of E_B/N_0. The region in which the matched-filtered two-bit demodulator performs better than its one-bit counterpart may be extended by using a nonzero detection threshold, as suggested in [2].

Figure 2-12 shows the optimal values of BT used for one- and two-bit Gaussian demodulators in Figure 2-11. As expected, filter bandwidth declines as channel noise power increases. Optimal BT values for the two demodulator structures are very close at all BER values considered. From Figures 2-7 and 2-10, it can be observed that both demodulator structures are fairly robust to BT values in the general vicinity of the optimum. Overly narrow filter bandwidths at high SNRs cause the greatest degradation. In this instance, the one-bit demodulator is slightly more robust than the two-bit.

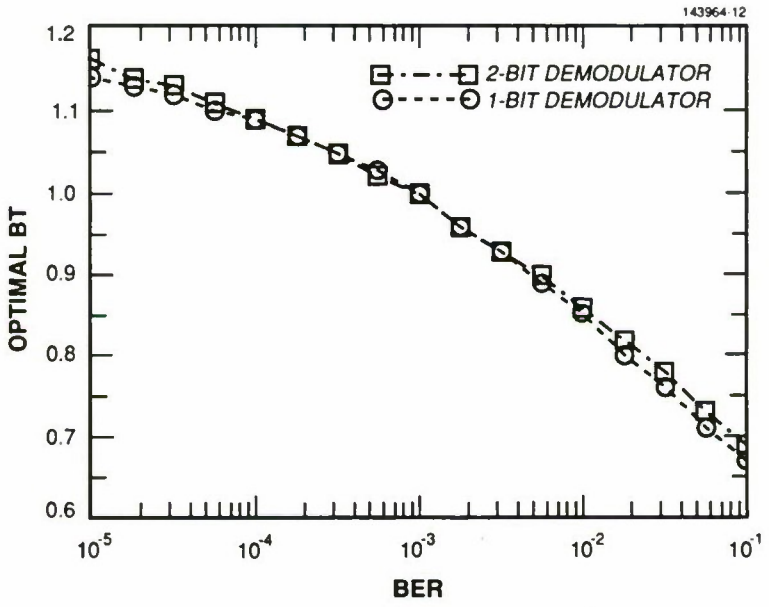

Figure 2-12. Optimized BT for Gaussian-filtered DMSK demodulators.

3. DPSK CROSS SUPPORT

3.1 DPSK Matched-Filtered Demodulators

Using complex notation, the standard PSK signal can be modeled as

$$e(t) = Re\left\{(u_P(t) + z(t))e^{j(\omega_c t+\theta)}\right\} \tag{3.1}$$

where $u_P(t)$ is the equivalent PSK baseband signal. Other variables are as defined in Section 2.1 for the MSK signal. The DPSK baseband equivalent signal with data rate $1/T$ bits/sec is given by

$$u_P(t) = \sqrt{2P}\sum_k d_k p\left((t - kT)/T\right) \tag{3.2}$$

where $p(x)$ is a rectangular baseband pulse of duration one centered at the origin:

$$p(x) = \begin{cases} 1 & -1/2 \le x \le 1/2 \\ 0 & elsewhere. \end{cases} \tag{3.3}$$

The best known noncoherent demodulator for this signal in a nonstressed environment is the delay and multiply with a DPSK matched filter, as shown in Figure 3-1 [10]; Figure 3-1(a) is an IF version of the demodulator, and Figure 3-1(b) is an equivalent baseband version. In the IF demodulator, the received signal passes through a bandpass matched filter with equivalent baseband impulse response $p(t/T)$. The filtered signal is multiplied by a delayed, conjugated version of itself, and the real part of the resulting product is hard-limited to provide estimates of the differentially coded data stream, $d_k d_{k-1}$. The delay and multiply function translates the signal to baseband and removes unknown phase.

Theoretical BER for an ideal DPSK matched-filter demodulator in AWGN with spectrum density $N_0/2$ is known to be [10]

$$P_e = \frac{1}{2}e^{-E_B/N_0} \tag{3.4}$$

where $E_B = PT$ is the energy per channel bit.

There are several important differences between Equations (3.2) and (2.2) that affect demodulator structure and performance: MSK has a half-cosine pulse shape versus a rectangular pulse for PSK; data are modulated onto both the in-phase and quadrature components of the MSK carrier, and each even- (odd-) numbered MSK pulse overlaps in time with the preceding and following odd- (even-) numbered pulses on the quadrature (in-phase) carrier component.

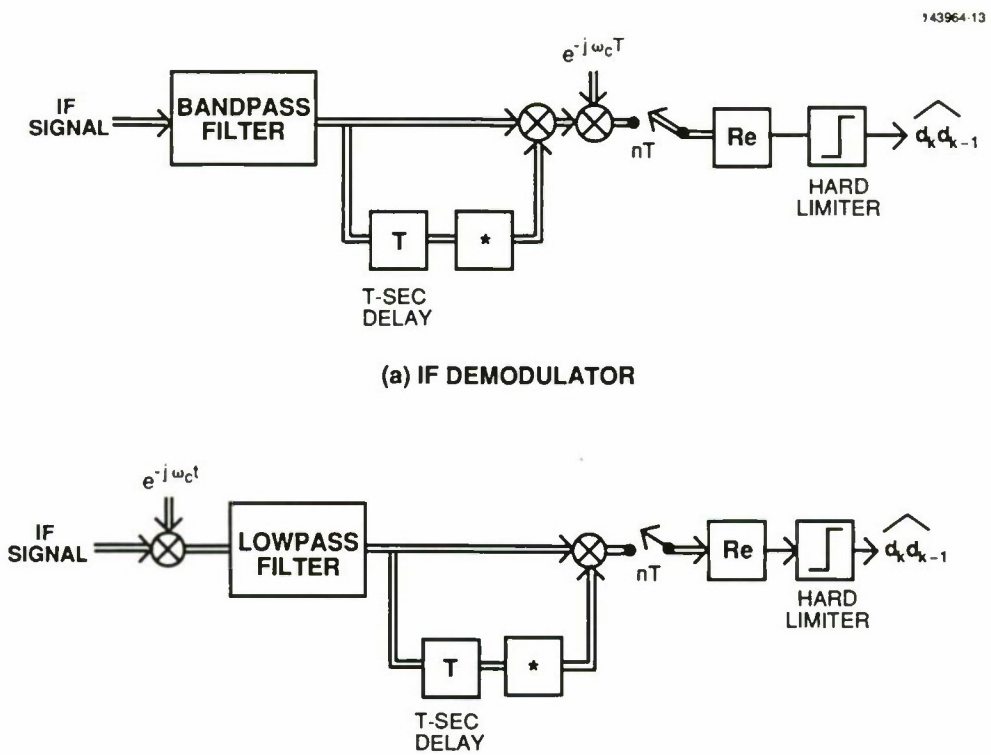

Figure 3-1. DPSK delay and multiply demodulator.

3.2 DPSK Cross Support Demodulators

It is desired to use a DMSK demodulator to receive DPSK signals. Comparing Figure 3-1 with Figures 2-1 and 2-2, it is evident that the baseband DPSK demodulator comprises a subset of the two-bit DMSK demodulator. Alternatively, it can be observed that the PSK equivalent baseband signal [Equation (3.2)] resembles the in-phase component of the equivalent baseband MSK signal [Equation (2.2)]. Because symbols on the in-phase and quadrature channels are multiplied together in the one-bit DMSK demodulator, it is not suitable for cross support of DPSK signals, which do not have a quadrature channel. However, the two-bit DMSK demodulator effectively demodulates each channel independently and may be used to receive DPSK signals with one-half the data rate of the intended DMSK signal.

The DPSK signal of interest is given by Equation (3.1) with $u_P(t)$ replaced by the equivalent baseband signal

$$u_C = \sqrt{2P} \sum_k d_k p\left(\frac{t - 2kT}{2T}\right) \tag{3.5}$$

where 1/T is the DMSK data rate. This signal has data rate $1/2T$. The symbol pulse, $p(t/2T)$, is as defined in Equation (3.3) except for the new factor of 1/2 in the argument and a duration of $2T$ sec. Defined this way, the DPSK signal is identical in form to the in-phase component of the DMSK signal, except for the symbol pulse shape.

DMSK receivers that have been configured for cross support of DPSK signals are illustrated in Figure 3-2. The IF demodulator is configured by reducing the sampling rate at the multiplier output by a factor of two. Samples that correspond to the DMSK in-phase channel are taken, and samples that correspond to the DMSK quadrature channel are ignored. An alternative view of reconfiguration is shown for the baseband demodulator structure, in which the lower (quadrature) signal path has been disconnected from the decision circuit. In effect, the two-bit DMSK demodulator is now acting as a "one-bit" delay and multiply demodulator for a DPSK signal with bit period twice that of the original DMSK signal.

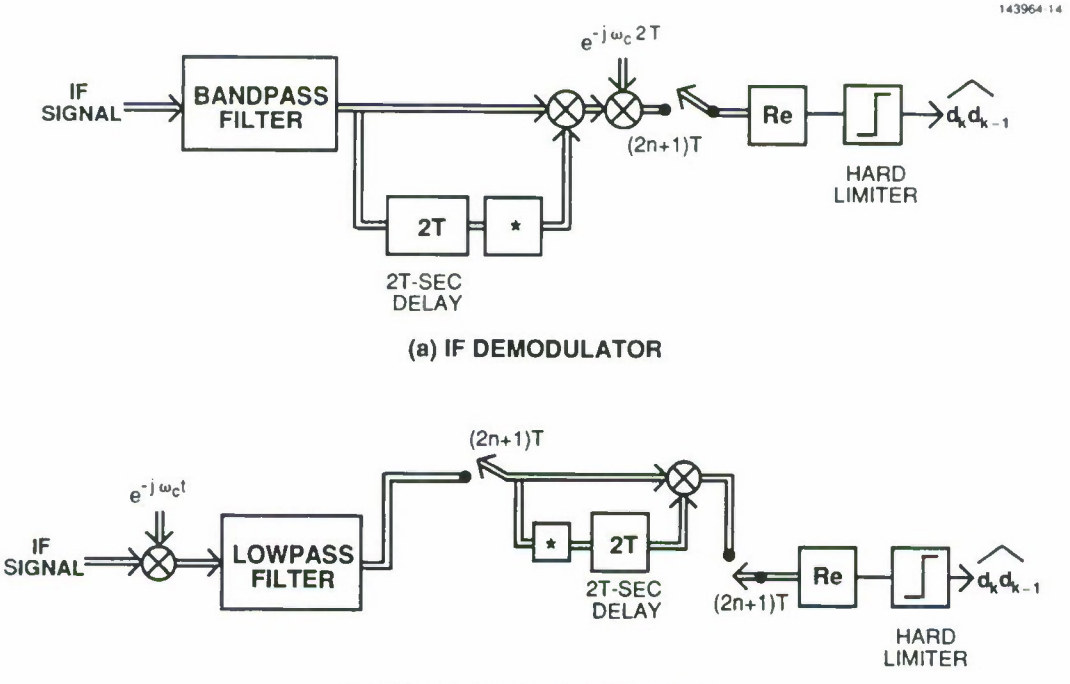

Figure 3-2. Two-bit DMSK demodulator configured for DPSK cross support.

Because detection filters are chosen to provide good performance with MSK signals, cross support provides suboptimal DPSK reception. In order to assess the reduction in DPSK performance with cross support, it is necessary to find the resulting BER for each DMSK detection filter.

3.3 Matched Filters

Given a cross support demodulator with the matched filters of Equation (2.5), the filtered PSK signal pulse will be

$$C_M(t) = \int_{-\infty}^{\infty} \widetilde{\cos}\left(\frac{\pi\tau}{2T}\right) p\left(\frac{t-\tau}{2T}\right) d\tau, \tag{3.6}$$

which is easily evaluated to be

$$C_M(t) = \begin{cases} \frac{2T}{\pi}\left(1+\cos\frac{\pi t}{2T}\right) & -2T < t < 2T \\ 0 & elsewhere. \end{cases} \tag{3.7}$$

The filtered pulse is a raised cosine with maximum amplitude $4T/\pi$ at $t = 0$ and duration $4T$. Because symbols are transmitted $2T$ sec apart, there is no ISI in the filtered signal. Figure 3-3 shows the matched-filtered PSK pulse normalized by $4T/\pi$.

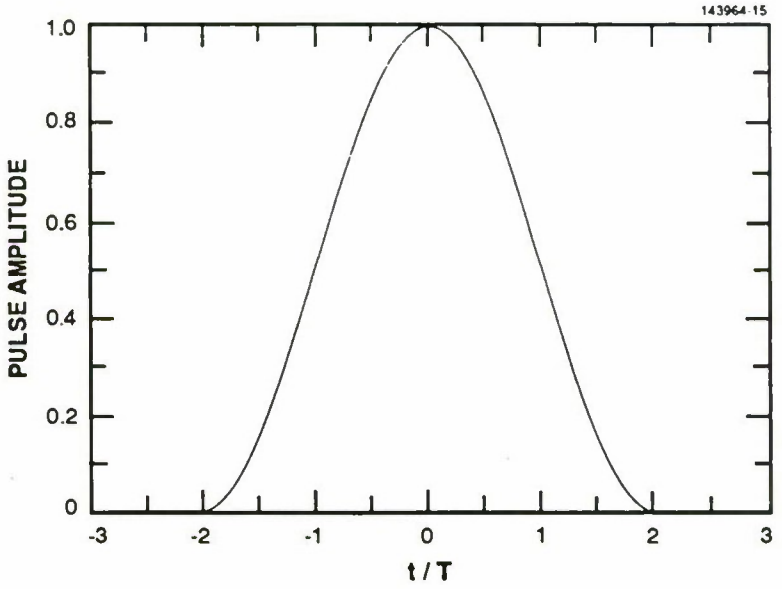

Figure 3-3. PSK cross support matched-filtered symbol pulse.

The filtered noise autocorrelation function is given by Equation (2.11), with noise power $\sigma^2 = N_0 T$. The noise autocorrelation is zero for samples spaced $2T$ sec or farther apart.

3.4 Gaussian Filters

The filtered PSK pulse in a Gaussian-filtered demodulator is

$$C_G(t) = \frac{k_1 B}{\pi} \int_{-\infty}^{\infty} e^{-(k_1 B\tau)^2} p\left(\frac{t-\tau}{2T}\right) d\tau. \tag{3.8}$$

This integral can be expressed in terms of the Gaussian error function as

$$C_G(t) = \frac{1}{2}\text{erf}\left[k_1 BT(1+t/T)\right] + \frac{1}{2}\text{erf}\left[k_1 BT(1-t/T)\right]. \tag{3.9}$$

The Gaussian-filtered PSK symbol pulse is graphed in Figure 3-4. This pulse is nonzero on an infinitely wide region, but falls off rapidly.

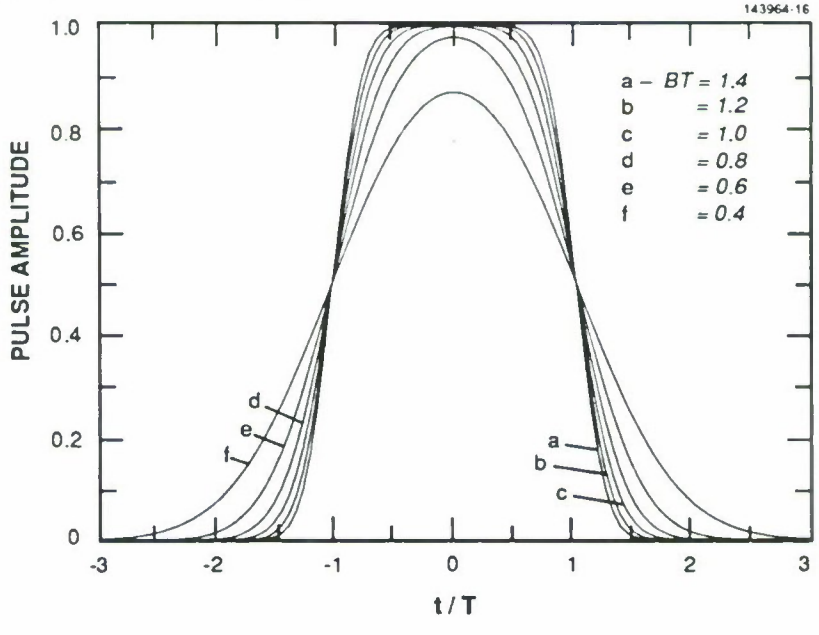

Figure 3-4. PSK Gaussian-filtered symbol pulse.

The Gaussian-filtered noise autocorrelation function is given by Equation (2.18). For BT $\geq$ 0.4, noise autocorrelation of samples taken $2T$ sec apart is $< 0.102R_G(0)$ and can be ignored when calculating demodulator BER performance.

3.5 Cross Support Performance

The DPSK cross support equivalent baseband filtered signal is

$$v(t) = \sqrt{2P}\sum_k d_k C(t-2kT) + n(t). \tag{3.10}$$

Demodulators equipped with MSK matched filters do not produce ISI in the filtered signal. Input signals to the multiplier at time $t = 2kT$ are

$$v(2kT) = \sqrt{2P} d_k \frac{4T}{\pi} + n_M(2kT) \tag{3.11}$$

and the complex conjugate of

$$v(2(k-1)T) = \sqrt{2P} d_{k-1} \frac{4T}{\pi} + n_M(2(k-1)T). \tag{3.12}$$

This signal pair, with no ISI and uncorrelated noise, resembles ordinary DPSK reception with signal amplitude $\sqrt{2P}\,4T/\pi$ and noise power N_0T. Keeping in mind that energy per channel bit is $2TP$, the BER for this demodulator is

$$P_e = \frac{1}{2} e^{-\frac{E_B}{N_0}\frac{8}{\pi^2}} \tag{3.13}$$

for a performance loss of $8/\pi^2 = 0.912$ dB relative to the delay and multiply demodulator with a DPSK matched filter.

When deriving BER for a DPSK cross support demodulator with a Gaussian filter, it is necessary to include ISI from adjacent symbols, even though they are spaced $2T$ sec apart. Partly, this results from heavier tails on the Gaussian-filtered PSK pulse compared to the filtered MSK pulse. Mostly, it is important to include ISI because otherwise the derived cross support BER expression results in a low value of the optimal BT, at which ISI does have a noticeable impact on demodulator performance. With the effects of ISI included in the BER expression, the optimal BT is large enough to ignore noise correlation for $\tau \geq 2T$ sec.

At time $t = 2kT$, equivalent baseband signals entering the multiplier of the Gaussian-filtered demodulator are

$$v(2kT) = \sqrt{2P}\,[d_k C_G(0) + (d_{k-1} + d_{k+1}) C_G(2T)] + n_G(2kT) \tag{3.14}$$

and the complex conjugate of

$$v(2(k-1)T) = \sqrt{2P}\,[d_{k-1} C_G(0) + (d_{k-2} + d_k) C_G(2T)] + n_G(2(k-1)T). \tag{3.15}$$

The resulting decision variable at the multiplier output is

$$\begin{aligned} v(2kT)v^*(2(k-1)T) = 2P \Big\{ & d_k d_{k-1} C_G^2(0) \\ & + C_G^2(2T)(d_{k-1} + d_{k+1})(d_{k-2} + d_k) \\ & + C_G(0) C_G(2T)\,[d_k(d_{k-2} + d_k) + d_{k-1}(d_{k-1} + d_{k+1})]\Big\} \\ & + noise. \end{aligned} \tag{3.16}$$

This decision variable is entirely real. Figure 3-5 illustrates the decision variable constellation. The probability of each constellation point occurring is listed in Table 3-1, assuming that data are independent and take on values ± 1 with equal probability.

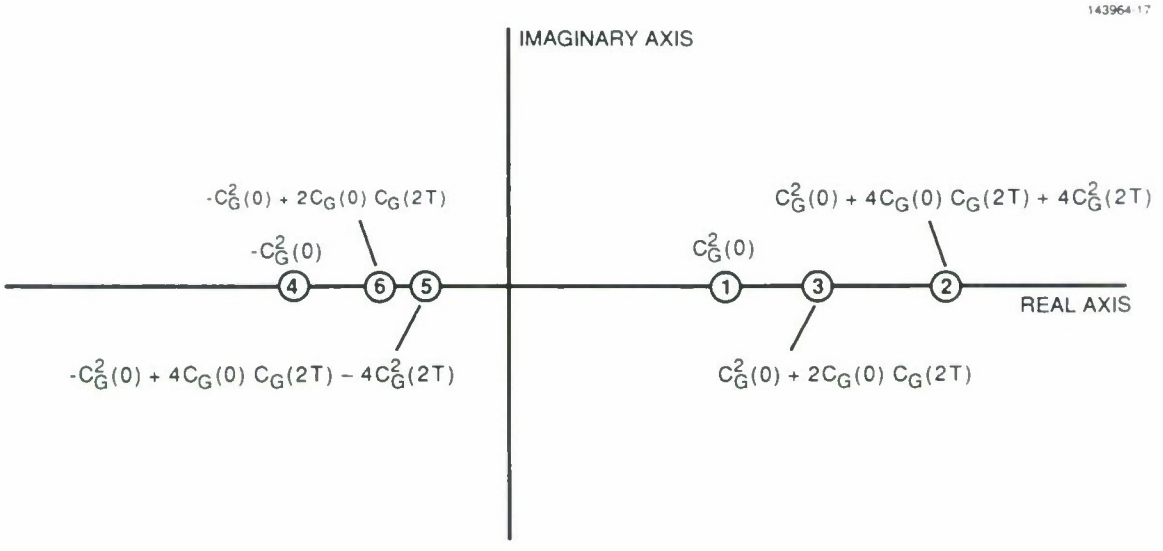

Figure 3-5. DPSK cross support constellation.

TABLE 3-1.

DPSK Cross Support Constellation Probabilities

Correct Decision	Constellation Point	Data Values	Probability
$d_k = d_{k-1}$:	1	$d_{k-2} + d_k = d_{k-1} + d_{k+1} = 0$	1/8
	2	$d_{k-2} + d_k = d_{k-1} + d_{k+1} = \pm 2$	1/8
	3	$d_{k-2} + d_k = 0,\ d_{k-1} + d_{k+1} = \pm 2$	1/8
	3	$d_{k-2} + d_k = \pm 2,\ d_{k-1} + d_{k+1} = 0$	1/8
$d_k \neq d_{k-1}$:	4	$d_{k-2} + d_k = d_{k-1} + d_{k+1} = 0$	1/8
	5	$d_{k-2} + d_k = -(d_{k-1} + d_{k+1}) = \pm 2$	1/8
	6	$d_{k-2} + d_k = 0,\ d_{k-1} + d_{k+1} = \pm 2$	1/8
	6	$d_{k-2} + d_k = \pm 2,\ d_{k-1} + d_{k+1} = 0$	1/8

Error probability is found in the Appendix for each constellation point; averaging error probability over constellation points produces the BER expression

$$P_e = \frac{1}{4} + \frac{1}{8}\left\{ e^{-\frac{E_B}{N_0}\frac{\sqrt{2\pi}\,C_G^2(0)}{k_1 2BT}} \left[1 + e^{-\frac{E_B}{N_0}\frac{\sqrt{2\pi}\,4C_G^2(2T)}{k_1 2BT}} \cosh\left(\frac{E_B}{N_0}\frac{\sqrt{2\pi}\,4C_G(0)C_G(2T)}{k_1 2BT} \right) \right] \right\}$$

$$+ \frac{1}{8}Q\left(\sqrt{\frac{E_B}{N_0}\frac{2\sqrt{2\pi}}{k_1 2BT}}\,C_G(2T),\ \sqrt{\frac{E_B}{N_0}\frac{2\sqrt{2\pi}}{k_1 2BT}}\,(C_G(0)+C_G(2T))\right)$$

$$- \frac{1}{8}Q\left(\sqrt{\frac{E_B}{N_0}\frac{2\sqrt{2\pi}}{k_1 2BT}}\,(C_G(0)+C_G(2T)),\ \sqrt{\frac{E_B}{N_0}\frac{2\sqrt{2\pi}}{k_1 2BT}}\,C_G(2T)\right)$$

$$+ \frac{1}{8}Q\left(\sqrt{\frac{E_B}{N_0}\frac{2\sqrt{2\pi}}{k_1 2BT}}\,C_G(2T),\ \sqrt{\frac{E_B}{N_0}\frac{2\sqrt{2\pi}}{k_1 2BT}}\,(C_G(0)-C_G(2T))\right)$$

$$- \frac{1}{8}Q\left(\sqrt{\frac{E_B}{N_0}\frac{2\sqrt{2\pi}}{k_1 2BT}}\,(C_G(0)-C_G(2T)),\ \sqrt{\frac{E_B}{N_0}\frac{2\sqrt{2\pi}}{k_1 2BT}}\,C_G(2T)\right) \tag{3.17}$$

where the ratio of detection filter bandwidth to data rate is 2BT.

Cross support performance is a function of detection filter bandwidth. Optimal BT can be found at each BER by searching over BT values to find that which requires the smallest E_B/N_0 to achieve the target BER. Optimal values of BT are listed in Table 3-2 for different BERs, along with the value of E_B/N_0 required to reach each BER with optimized BT. Required E_B/N_0 with a DPSK matched-filter demodulator is also listed in the Table, for purposes of comparison.

TABLE 3-2.

DPSK Cross Support Optimal BT

BER	DPSK Cross Support		DPSK Matched Filter
	Optimal BT	Required E_B/N_0 (dB)	Required E_B/N_0 (dB)
10^{-1}	0.41	2.70	2.07
10^{-2}	0.44	6.68	5.92
10^{-3}	0.46	8.77	7.93
10^{-4}	0.47	10.20	9.30
10^{-5}	0.48	11.28	10.34

Optimal values of BT are in the range 0.4 to 0.5 for all BERs considered, significantly lower than optimal BT for DMSK reception. Figure 3-6 shows DPSK cross support BER performance for different detection filters: Gaussian filters with BT optimized for DPSK cross support; with BT optimized for DMSK; with BT = 0.5 and 0.8; and with DMSK matched filters. BER results for a delay and multiply DPSK matched-filtered demodulator are also shown.

It is clear from the figure that choosing a detection filter for a DMSK demodulator that will provide cross support requires some thought. Cross support degradation using BT optimized for DPSK is less than 0.8 dB; however, DMSK performance will be degraded by 8.6 dB (BER = 0.01) at this bandwidth. Increasing BT only slightly, to 0.5, DPSK degradation is 0.9 dB and DMSK

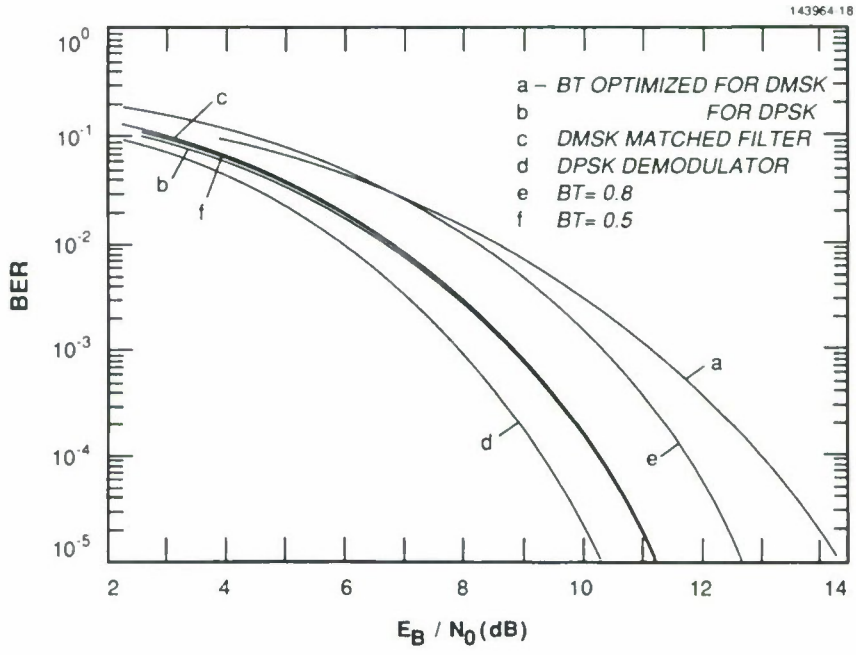

Figure 3-6. DPSK cross support performance.

degradation is 4.1 dB. Using BT optimized for DMSK results in 2.6 dB of cross support degradation, when BER = 0.01.

Cross support performance of optimized Gaussian-filtered demodulators, Gaussian-filtered demodulators with BT = 0.5, and DMSK matched-filtered demodulators is nearly indistinguishable in Figure 3-6. Their performance with DMSK signals is not so close. As noted above, DMSK performance with BT optimized for cross support is 4.5 dB worse than performance with BT = 0.5 at BER = 0.01. DMSK matched-filtered performance with a DMSK signal is degraded 1.7 dB. This suggests that if demodulator design is driven by DPSK cross support performance, a DMSK matched filter may be the best design choice. (DPSK matched filters are not suitable for DMSK demodulation.)

Observe that using a near-optimal value (for DMSK) of BT = 0.8, degradation for DPSK cross support is ≈2.3 dB, although using optimal (for DMSK) BT produces 2.6 dB of degradation. In this region, cross support performance is more sensitive to the value of BT than DMSK performance. Variable detection filter bandwidth in the Gaussian-filtered DMSK demodulator allows the designer to trade-off performance in the two modes of operation. BT can be set somewhere between the optimal values for DMSK and DPSK cross support, with the goal of providing good demodulator performance for both signals. The appropriate BT value depends on many factors, including performance requirements, constraints, and power costs for each transmitter/receiver pair. One possible scenario is that performance requirements, power costs, and duty cycles (not data volume) are identical for the two channels. Since the DPSK data rate is half that on the DMSK channel,

average signal power is proportional to

$$\left(\frac{E_B}{N_0}\right)_{DMSK} + \frac{1}{2}\left(\frac{E_B}{N_0}\right)_{DPSK}. \tag{3.18}$$

Optimal BT values are found as before, now minimizing Equation (3.18) for each BER. Results are tabulated in Table 3-3 and plotted in Figures 3-7 and 3-8. Figure 3-7 compares the jointly optimized BT product with optimal BTs for DMSK and DPSK cross support. This figure suggests that DMSK dominates the optimization process, producing BT values near the optimum for DMSK at most BERs. Figure 3-8 compares BER performance using jointly optimized BT with BER performance of receivers optimized for one signal. Comparing Figures 3-6 and 3-8, DPSK cross support with BER = 0.01 has improved 0.5 dB, relative to the demodulator optimized for DMSK, while DMSK performance has degraded 0.13 dB. With respect to a DPSK demodulator, cross support degradation is now 2.1 dB.

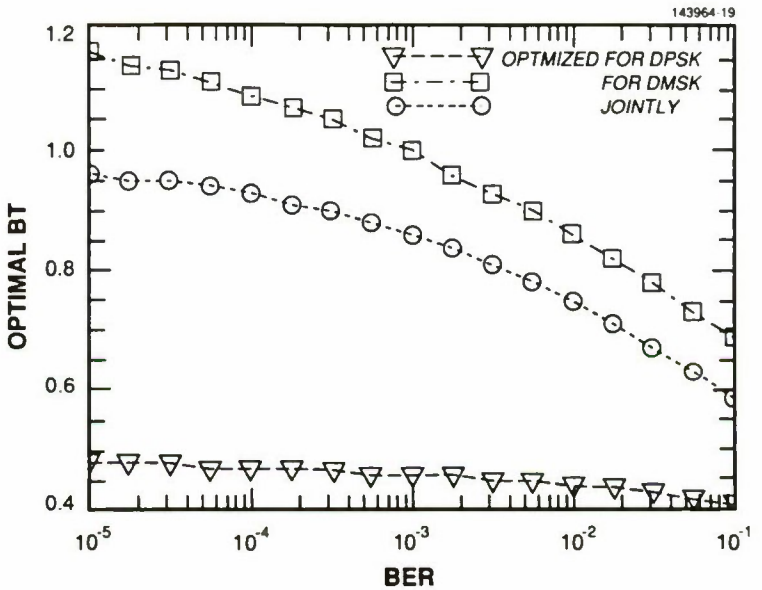

Figure 3-7. Jointly optimized BT for DMSK and DPSK cross support.

For different optimization cost functions, other values of BT may be chosen which produce comparable DMSK and DPSK degradation (relative to optimized DPSK cross support). However, Figures 3-6 and 2-10 show that reducing BT from the optimal value for DMSK by any significant quantity, results in DMSK performance degradation greater than the DPSK cross support performance degradation that results when BT is increased from the optimal value for DPSK cross support by the same amount. In short, ISI in the DMSK signal resulting from a too-narrow filter bandwidth is more deleterious than increased noise power in the DPSK signal from a too-wide filter bandwidth.

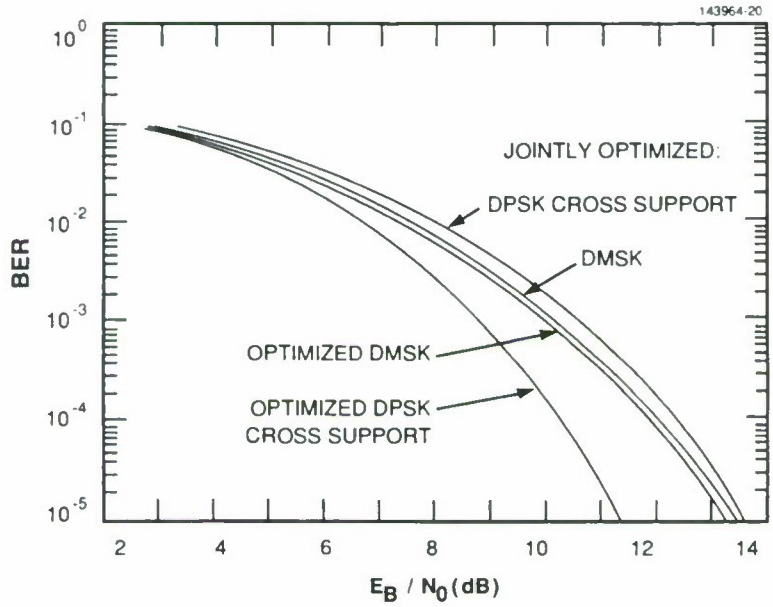

Figure 3-8. DMSK and DPSK Gaussian-filtered demodulator performance with jointly optimized BT.

TABLE 3-3.

Joint DMSK and DPSK Cross Support Optimal BT

BER	Optimal BT	DMSK Required E_B/N_0 (dB)	DPSK Cross Support Required E_B/N_0 (dB)
10^{-1}	0.59	2.92	3.29
10^{-2}	0.75	7.55	7.98
10^{-3}	0.86	10.15	10.58
10^{-4}	0.93	11.98	12.27
10^{-5}	0.96	13.37	13.45

4. CONCLUSIONS

This report summarizes the performance of DMSK demodulators for reception of either DMSK or DPSK signals based on analytical results for BER. Two DMSK structures were compared, the one- and the two-bit demodulators. Two types of detection filters were also considered, DMSK matched and narrowband (or lowpass) Gaussian filters. The importance of Gaussian filter bandwidth as a design variable was examined. Demodulator and filter types were explored in terms of performance with DMSK signals and suitability for receiving DPSK signals. Where applicable, demodulator performance when receiving DPSK signals was investigated.

The two-bit demodulator with Gaussian detection filter was found to be the most efficient DMSK demodulator of those considered. Filter bandwidth depends on the desired channel BER. For a wide range of BERs, 0.1 to 0.006, choosing BT = 0.8 results in nearly optimal performance. As BER declines, the optimal bandwidth will increase, reaching 1.16 for BER = 10^{-5}.

The DMSK two-bit demodulator can also be used for DPSK cross support at no cost in DMSK performance. The supported DPSK data rate is one-half that of the DMSK signal the demodulator was designed to receive. The one-bit DMSK demodulator was shown to be unsuitable for cross support.

Performance of DPSK cross support by a DMSK demodulator depends on the detection filter used. If the demodulator detection filter is chosen to optimize DMSK performance (under the constraint that it must be a matched or Gaussian filter), DPSK cross support performance at BER = 0.01 will degrade ≈2.6 dB relative to a delay and multiply DPSK demodulator with a DPSK matched filter, and larger penalties will be incurred as BER declines. If the detection filter is chosen to optimize DPSK cross support performance (under the same constraints), then BT = 0.44 and cross support degradation will be less than 0.8 dB; however, DMSK performance will degrade 8.6 dB. Even a small backoff of BT from the optimal cross support value will drastically reduce DMSK degradation; for BT = 0.5, DMSK degradation is 4.1 dB. DMSK matched filters provide cross support performance equivalent to Gaussian filters optimized for cross support, with a reduced penalty in DMSK performance: 1.7 dB relative to optimized Gaussian filter performance. For systems whose design is driven by cross support requirements, matched filters are probably the best choice.

The possibility of using a detection filter bandwidth between the optimal values for DMSK and DPSK cross support was also investigated. The criterion used was to minimize transmitter power, assuming that both waveforms have equal duty cycles and performance requirements. The resulting jointly optimized transmitter power requirements are close to those of optimal DMSK, however DPSK cross support performance is degraded ≈2.1 dB versus 2.6 dB with optimal DMSK performance. Jointly optimized BT values are fairly close to BT optimized for DMSK. Since DMSK requires greater transmitter power to reach a specified performance level, it is not surprising that DMSK BER dominated the optimization process. It is likely that most reasonable choices for weights in the optimization function will have similar results, dominated by DMSK performance requirements.

APPENDIX A
DMSK DEMODULATOR PERFORMANCE

A.1 Introduction

In this Appendix BER expressions are derived for the different DMSK receivers with DMSK and DPSK signals. BER derivations are based on the results of Stein [8,9] for differential detection of general binary PSK signals. Results differ for each demodulator as a result of differing constellations, filtered pulse shapes, and noise correlation. General principles are outlined in the next section, and particular results for each demodulator follow.

A.2 General Formulation

In deriving BER expressions for DMSK demodulators, the following assumptions are made:

1. Interference is AWGN, with PSD $N_0/2$;
2. Channel bits are mutually independent, and take on value ± 1 with equal probability;
3. Gaussian filters are ideal (unrealizable);
4. ISI results only from immediately adjacent symbols; and
5. Filtered noise autocorrelation $R(\tau) \approx 0$ for $\tau \geq 2T$.

In the Gaussian-filtered case, assumptions 4 and 5 depend on filter bandwidth; however, filters that provide good quality reception are consistent with these assumptions.

In order to use [8,9], equivalent baseband-filtered signals are written in polar form. The two filtered signals, the product of which is the basis for a decision at time $t = kT$, are expressed as

$$v(kT) = A_k d_k e^{j\theta_k} + n(kT) \tag{A.1}$$

and

$$v(lT) = A_l d_l e^{j\theta_l} + n(lT) \tag{A.2}$$

where $l = k - 1$ or $k - 2$ for the one- and two-bit demodulators, respectively. Equations (A.1) and (A.2) describe symbol samples at the ideal sampling instant, when both symbols are at their maximum amplitudes. Phase angles, θ, reflect displacement of the samples from their ideal locations on the real axis due to ISI and are limited to $-\pi/2 \leq \theta \leq \pi/2$.

Assumption 4 allows the polar form signal parameters of Equation (A.1) to be written as

$$A_k = \sqrt{2P}\left(S^2(0) + S^2(T)(d_{k-1} + d_{k+1})^2\right)^{1/2} \tag{A.3}$$

and

$$\theta_k = -\arctan\left(\frac{(d_{k-1} + d_{k+1})S(T)}{d_k S(0)}\right) \tag{A.4}$$

where arctan(·) is the principal value of the inverse tangent, in the range $-\pi/2 \leq \theta \leq \pi/2$.

With $l = k - 1$, the polar form parameters of the delayed signals in the one-bit demodulator are (absorbing j into the expression)

$$A_{k-1} = \sqrt{2P}\left(S^2(0) + (d_{k-2} + d_k)^2 S^2(T)\right)^{1/2} \tag{A.5}$$

$$\theta_{k-1} = \arctan\left(\frac{(d_{k-2} + d_k)S(T)}{d_{k-1}S(0)}\right). \tag{A.6}$$

With $l = k - 2$, polar form parameters for the delayed signal in the two-bit demodulator are

$$A_{k-2} = \sqrt{2P}\left(S^2(0) + (d_{k-3} + d_{k-1})^2 S^2(T)\right)^{1/2} \tag{A.7}$$

$$\theta_{k-2} = -\arctan\left(\frac{(d_{k-3} + d_{k-1})S(T)}{d_{k-2}S(0)}\right). \tag{A.8}$$

Noise samples in Equations (A.1) and (A.2) have autocorrelation

$$R(kT - lT) = \sigma^2(\rho_c + j\rho_s). \tag{A.9}$$

Using matched filters, noise power is

$$\sigma^2 = N_0 T \tag{A.10}$$

and covariance in the one-bit demodulator is

$$\begin{aligned} \rho_c &= 0 \\ \rho_s &= -1/\pi \end{aligned} \tag{A.11}$$

which includes the effects of the factor j in the delay branch. Noise covariance in the matched-filtered two-bit demodulator is

$$\rho_c = 0 \tag{A.12}$$

$$\rho_s = 0. \tag{A.13}$$

With a Gaussian detection filter, the parameters of Equation (A.9) are, for both receivers:

$$\sigma^2 = \frac{k_1 N_0 B}{\sqrt{2\pi}} \tag{A.14}$$

where k_1 is the Gaussian filter bandwidth normalizing coefficient defined in Section 2.3 ($k_1 = \pi/\sqrt{2\log(2)}$). For the one-bit demodulator:

$$\begin{aligned} \rho_c &= 0 \\ \rho_s &= -e^{-(k_1 BT)^2/2} \end{aligned} \tag{A.15}$$

and for the two-bit demodulator:

$$\begin{aligned} \rho_c &= e^{-2(k_1 BT)^2} \approx 0 \\ \rho_s &= 0. \end{aligned} \tag{A.16}$$

Detector output is the sign of $Re\{v(kT)v^*(lT)\}$. When $d_k = d_l$, the probability of error is the probability that

$$Re\{v(kT)v^*(lT)\} < 0. \tag{A.17}$$

In the most general case, with $A_k \neq A_l$, $\theta_k \neq \theta_l$, and nonzero noise covariance, the probability of error for $d_k = d_l$ is [8,9]

$$P_e = \frac{1+A}{2}\left(1 - Q(\sqrt{b}, \sqrt{a})\right) + \frac{1-A}{2} Q(\sqrt{a}, \sqrt{b}) \tag{A.18}$$

where $Q(\cdot,\cdot)$ is Marcum's Q-function, and the BER parameters are

$$A = \frac{\rho_c}{\sqrt{1-\rho_s^2}} \tag{A.19}$$

$$\begin{aligned} \left\{ \begin{array}{c} a \\ b \end{array} \right\} = \frac{1}{4\sigma^2(1-\rho_s^2)} \Big(& A_k^2 + A_l^2 + 2\rho_s A_k A_l \sin(\theta_l - \theta_k) \\ & \left\{ \begin{array}{c} - \\ + \end{array} \right\} 2\sqrt{1-\rho_s^2} A_k A_l \cos(\theta_l - \theta_k) \Big). \end{aligned} \tag{A.20}$$

It is easy to verify that right half-plane constellation points, which are symmetric across the real axis, produce the same BER. This is the justification for lumping such points together in the two-bit demodulator constellation of Figure 2-8.

When the signal constellation is symmetric about the imaginary axis, conditional BER for the cases $d_k = d_l$ and $d_k \neq d_l$ are identical; only right half-plane constellation points need to be considered in finding the BER. When the constellation is not symmetric, conditional BER due to left half-plane constellation points must be found separately.

In order to use Equations (A.17) through (A.20) to find the conditional error probabilities associated with constellation points in the left half-plane, the problem will be transformed into

one for which Equation (A.17) is the error condition. When $d_k \neq d_l$ the probability of error is the probability that the real part of $v(kT)v^*(lT)$ is greater than zero. Multiplying all terms in the error condition by -1 produces an error condition similar to Equation (A.17). The minus sign on the left side of this condition can be absorbed into the value of the delayed sample, which is redefined to be

$$\tilde{v}(lT) = (-d_l)A_l e^{j\theta_l} + \tilde{n}(lT) \tag{A.21}$$

where

$$\tilde{n}(lT) = -n(lT), \tag{A.22}$$

and the error condition is now

$$Re\left\{v(kT)\tilde{v}^*(lT)\right\} > 0. \tag{A.23}$$

This is a binary DPSK system with $d_k = (-d_l)$; A_k, A_l, θ_k, θ_l, and σ^2 are defined as before, and noise covariance

$$\tilde{\rho}_c = -\rho_c \tag{A.24}$$

$$\tilde{\rho}_s = -\rho_s. \tag{A.25}$$

In terms of the original signal parameters, the conditional BER for $d_k \neq d_l$ is given by Equation (A.18) with

$$A = \frac{-\rho_c}{\sqrt{1+\rho_s^2}} \tag{A.26}$$

$$\left\{ \begin{array}{c} a \\ b \end{array} \right\} = \frac{1}{4\sigma^2(1-\rho_s^2)} \left(A_k^2 + A_l^2 - 2\rho_s A_k A_l \sin(\theta_l - \theta_k) \right.$$

$$\left. \left\{ \begin{array}{c} - \\ + \end{array} \right\} 2\sqrt{1-\rho_s^2} A_k A_l \cos(\theta_l - \theta_k) \right). \tag{A.27}$$

For each receiver, signal amplitudes and angles will vary from sample to sample due to ISI. The BER must be found for each possible ISI pattern, then averaged over ISI using assumption 2. Assumption 4 serves to limit the number of ISI patterns that must be considered.

A.3 The Gaussian-Filtered One-Bit Demodulator

The Gaussian-filtered one-bit demodulator has a symmetric constellation, so that the average BER is equal to the BER for the case $d_k = d_{k-1}$. Constellation probabilities in the average are modified to reflect the fact that they are conditional on $d_k = d_{k-1}$.

Filtered noise correlation is given by Equations (A.14) and (A.15). For these values Equation (A.19) becomes A = 0. Using the noise correlation with Equations (A.3) through (A.6), and defining $E_B = PT$, BER parameters for the three right half-plane constellation points are:

Point 1: $d_{k-2} + d_k = d_{k-1} + d_{k+1} = 0$ with probability 1/4

$$A_k = A_{k-1} = \sqrt{2P}\, S_G(0) \tag{A.28}$$

$$\theta_k = \theta_{k-1} = 0. \tag{A.29}$$

Equation (A.20) simplifies to

$$\left\{ \begin{array}{c} a_1 \\ b_1 \end{array} \right\} = \frac{E_B}{N_0} \frac{\sqrt{2\pi}}{2k_1 BT} \left(\frac{S_G(0)}{\sqrt{1 - e^{-(k_1 BT)^2/2}}} \left\{ \begin{array}{c} - \\ + \end{array} \right\} \frac{S_G(0)}{\sqrt{1 + e^{-(k_1 BT)^2/2}}} \right)^2 . \tag{A.30}$$

Point 2: $d_{k-2} + d_k = d_{k-1} + d_{k+1} = \pm 2$ with probability 1/4

$$A_k = A_{k-1} = \sqrt{2P} \left[S_G^2(0) + 4S_G^2(T) \right]^{1/2} \tag{A.31}$$

$$\theta_k = -\theta_{k-1} = -\arctan(\, 2S_G(T)/S_G(0)\,) \tag{A.32}$$

and a_2 and b_2 become

$$\left\{ \begin{array}{c} a_2 \\ b_2 \end{array} \right\} = \frac{E_B}{N_0} \frac{\sqrt{2\pi}}{2k_1 BT} \left(\frac{S_G(0) + 2S_G(T)}{\sqrt{1 - e^{-(k_1 BT)^2/2}}} \left\{ \begin{array}{c} - \\ + \end{array} \right\} \frac{S_G(0) - 2S_G(T)}{\sqrt{1 + e^{-(k_1 BT)^2/2}}} \right)^2 . \tag{A.33}$$

Point 3: $d_{k-2} + d_k \neq d_{k-1} + d_{k+1}$ with probability 1/2. Without loss of generality assume that $d_{k-2} + d_k = 0$ and $d_{k-1} + d_{k+1} = \pm 2$, for which

$$A_k = \sqrt{2P} \left[S_G^2(0) + 4S_G^2(T) \right]^{1/2} \tag{A.34}$$

$$A_{k-1} = \sqrt{2P}\, S_G(0) \tag{A.35}$$

$$\theta_k = -\arctan(\, 2S_G(T)/S_G(0)\,) \tag{A.36}$$

$$\theta_{k-1} = 0. \tag{A.37}$$

BER parameters can be simplified to

$$\left\{ \begin{array}{c} a_3 \\ b_3 \end{array} \right\} = \frac{1}{2} \left\{ \begin{array}{c} a_1 \\ b_1 \end{array} \right\} + \frac{1}{2} \left\{ \begin{array}{c} a_2 \\ b_2 \end{array} \right\} \left\{ \begin{array}{c} - \\ + \end{array} \right\} \frac{E_B}{N_0} \frac{2\sqrt{2\pi}}{k_1 BT} \frac{S_G(T)^2}{\sqrt{1 - e^{-(k_1 BT)^2}}}. \tag{A.38}$$

Averaging over these three cases gives the BER expression of Equation (2.23).

A.4 The Matched-Filtered One-Bit Demodulator

BER for the matched-filtered one-bit demodulator is found exactly as for the Gaussian-filtered. Here noise correlation is given by Equations (A.10) and (A.11), and symbol samples are $S_M(0) = T$ and $S_M(T) = T/\pi$. Conditional BER expressions can be found from the Gaussian-filtered case by replacing $S_G(\cdot)$ with $S_M(\cdot)$, $N_0 k_1 B/\sqrt{2\pi}$ with $N_0 T$, and $-\exp(-(k_1 BT)^2/2)$ with $-1/\pi$. Defining $c = \pi^2/(\pi^2 - 1) \approx 1.1127$, expressions can be simplified to the forms listed here:

Point 1: $d_{k-2} + d_k = d_{k-1} + d_{k+1} = 0$ with probability 1/4

$$a_1 = \frac{E_B}{N_0} c \left(1 - \frac{1}{\sqrt{c}}\right) \tag{A.39}$$

$$b_1 = \frac{E_B}{N_0} c \left(1 + \frac{1}{\sqrt{c}}\right). \tag{A.40}$$

Point 2: $d_{k-2} + d_k = d_{k-1} + d_{k+1} = \pm 2$ with probability 1/4

$$a_1 = \frac{E_B}{N_0} c \left(1 - \frac{1 - 4/\pi^2}{\sqrt{c}}\right) \tag{A.41}$$

$$b_1 = \frac{E_B}{N_0} c \left(1 + \frac{1 - 4/\pi^2}{\sqrt{c}}\right). \tag{A.42}$$

Point 3: $d_{k-2} + d_k \neq d_{k-1} + d_{k+1}$ with probability 1/2

$$a_3 = \frac{E_B}{N_0} c \left(1 - \frac{1}{\sqrt{c}}\right) \tag{A.43}$$

$$b_3 = \frac{E_B}{N_0} c \left(1 + \frac{1}{\sqrt{c}}\right) \tag{A.44}$$

which is identical to Point 1.

Averaging over these three cases gives the BER expression of Equation (2.22).

A.5 The Gaussian-Filtered Two-Bit Demodulator

The Gaussian-filtered two-bit demodulator constellation is asymmetric about the imaginary axis, and the cases $d_k = d_{k-2}$ and $d_k \neq d_{k-2}$ must both be considered when deriving the BER.

Filtered noise autocorrelation is given by Equations (A.14) and (A.16). With the two symbol delay, noise correlation between multiplier input signals is very small and is assumed to be zero. Using $\rho_c = 0$, Equation (A.19) becomes A = 0.

For $d_k = d_{k-2}$:

Point 1: $d_{k-3} + d_{k-1} = d_{k-1} + d_{k+1} = 0$ with probability 1/8

$$A_k = \quad A_{k-2} = \quad \sqrt{2P}\, S_G(0) \tag{A.45}$$

$$\theta_k = \quad \theta_{k-2} = \quad 0. \tag{A.46}$$

With equal input signals and uncorrelated noise, this case simplifies to that of DPSK with signal to noise ratio $A_k^2/2\sigma^2$ [8,9]. Using $E_B/N_0 = PT$

$$BER(1) = \frac{1}{2} e^{-\frac{E_B}{N_0} \frac{\sqrt{2\pi}\, S_G^2(0)}{k_1 BT}}. \tag{A.47}$$

Point 2: $d_{k-3} + d_{k-1} = d_{k-1} + d_{k+1} = \pm 2$ with probability 1/8

$$A_k = \quad A_{k-2} = \quad \sqrt{2P} \left[S_G^2(0) + 4S_G^2(T) \right]^{1/2} \tag{A.48}$$

$$\theta_k = \quad \theta_{k-2} = \quad -\arctan(\, 2S_G(T)/S_G(0)\,). \tag{A.49}$$

Input signals are equal, but with a slightly greater amplitude than the previous case. BER for this case reduces to

$$BER(2) = \frac{1}{2} e^{-\frac{E_B}{N_0} \frac{\sqrt{2\pi}}{k_1 BT} \left(S_G^2(0) + 4S_G^2(T) \right)}. \tag{A.50}$$

Point 3: $d_{k-3} + d_{k-1} \neq d_{k-1} + d_{k+1}$ with probability 1/4. Without loss of generality assume that $d_{k-3} + d_{k-1} = 0$, and $d_{k-1} + d_{k+1} = \pm 2$, for which

$$A_k = \sqrt{2P} \left[S_G^2(0) + 4S_G^2(T) \right]^{1/2} \tag{A.51}$$

$$A_{k-2} = \sqrt{2P}\, S_G(0) \tag{A.52}$$

$$\theta_k = \pm \arctan(\, 2S_G(T)/S_G(0)\,) \tag{A.53}$$

$$\theta_{k-2} = 0. \tag{A.54}$$

The parameters a and b simplify to

$$a_3 = \frac{E_B}{N_0} \frac{\sqrt{2\pi}}{k_1 BT} 2S_G^2(T) \tag{A.55}$$

$$b_3 = \frac{E_B}{N_0} \frac{\sqrt{2\pi}}{k_1 BT} \left(2S_G^2(0) + 2S_G^2(T) \right). \tag{A.56}$$

$d_k \neq d_{k-2}$: Here BER parameters are found from Equation (A.27). Most of the left half-plane points produce BER results identical to those of a previously considered right half-plane constellation point.

Point 4: $d_{k-3} + d_{k-1} = d_{k-1} + d_{k+1} = 0$ with probability 1/8. Signal parameters and BER are identical to point 1.

Point 5: $d_{k-3} + d_{k-1} = d_{k-1} + d_{k+1} = \pm 2$ with probability 1/8. Signal parameters are

$$A_k = \quad A_{k-2} = \quad \sqrt{2P}\left[S_G^2(0) + 4S_G^2(T)\right]^{1/2} \tag{A.57}$$

$$\theta_k = \quad -\theta_{k-2} = \quad \pm \arctan(\, 2S_G(T)/S_G(0)\,). \tag{A.58}$$

Using these relations in Equation (A.20), it becomes

$$a_5 \quad = \quad \frac{E_B}{N_0}\frac{\sqrt{2\pi}}{k_1 BT}\, 8S_G^2(T) \tag{A.59}$$

$$b_5 \quad = \quad \frac{E_B}{N_0}\frac{\sqrt{2\pi}}{k_1 BT}\, 2S_G^2(0). \tag{A.60}$$

Point 6: $d_{k-3} + d_{k-1} \neq d_{k-1} + d_{k+1}$ with probability 1/4. This point produces the same conditional BER as point 3.

Averaging over these six cases gives the BER expression Equation (2.27).

A.6 The Matched-Filtered Two-Bit Demodulator

An expression for BER in the matched-filtered two-bit demodulator is found as for the Gaussian-filtered. Noise power is given by Equation (A.10). As was assumed for the Gaussian-filtered signal, noise covariance between samples taken 2T sec apart is zero. Symbol samples are now $S_M(0) = T$ and $S_M(T) = T/\pi$. Conditional BER expressions can be found from those for the Gaussian-filtered case by replacing $S_G(\cdot)$ with $S_M(\cdot)$, and $N_0 k_1 B/\sqrt{2\pi}$ with $N_0 T$. After simplification, results are:

Point 1: $d_{k-3} + d_{k-1} = d_{k-1} + d_{k+1} = 0$ with probability 1/8

$$BER(1) = \frac{1}{2}e^{-E_B/N_0}. \tag{A.61}$$

Point 2: $d_{k-3} + d_{k-1} = d_{k-1} + d_{k+1} = \pm 2$ with probability 1/8

$$BER(2) = \frac{1}{2}e^{-\frac{E_B}{N_0}\left(1+\frac{4}{\pi^2}\right)}. \tag{A.62}$$

Point 3: $d_{k-3} + d_{k-1} \neq d_{k-1} + d_{k+1}$ with probability 1/4

$$a_3 \quad = \quad \frac{E_B}{N_0}\frac{2}{\pi^2} \tag{A.63}$$

$$b_3 \quad = \quad \frac{E_B}{N_0}\left(2 + \frac{2}{\pi^2}\right). \tag{A.64}$$

Point 4: $d_{k-3} + d_{k-1} = d_{k-1} + d_{k+1} = 0$ with probability 1/8. Identical to point 1.

Point 5: $d_{k-3} + d_{k-1} = d_{k-1} + d_{k+1} = \pm 2$ with probability 1/8.

$$a_5 = \frac{E_B}{N_0}\frac{8}{\pi^2} \tag{A.65}$$

$$b_5 = \frac{E_B}{N_0} 2. \tag{A.66}$$

Point 6: $d_{k-3} + d_{k-1} \neq d_{k-1} + d_{k+1}$ with probability 1/4. Results for this point are identical to point 3.

Averaging over these six cases gives the BER expression of Equation (2.26).

A.7 DPSK Cross Support Performance with Gaussian Filters

For DPSK cross support by a Gaussian-filtered two-bit demodulator, filtered noise power is given by Equation (A.14), and noise autocorrelation between adjacent symbols is assumed to be zero. Using $\rho = 0$ in Equation (A.19) gives A = 0. Using polar notation, the equivalent baseband symbols affecting a decision, sampled at the instant of peak amplitude, are

$$\begin{aligned} A_k &= \sqrt{2P}\,(C_G(0) + C_G(2T)(d_{k-1} + d_{k+1})/d_k) \\ \theta_k &= 0 \end{aligned} \tag{A.67}$$

and

$$\begin{aligned} A_{k-1} &= \sqrt{2P}\,(C_G(0) + C_G(2T)(d_{k-2} + d_k)/d_{k-1}) \\ \theta_{k-1} &= 0. \end{aligned} \tag{A.68}$$

Cross support is a special case of the general PSK problem solved by Equations (A.18) through (A.20), with purely real signal components and zero noise covariance. For this case, Equation (A.20) reduces to

$$\left\{ \begin{array}{c} a \\ b \end{array} \right\} = \frac{1}{4\sigma^2}\left(A_k \left\{ \begin{array}{c} - \\ + \end{array} \right\} A_l \right)^2. \tag{A.69}$$

When finding the conditional probabilities of error for $d_k = d_{k-1}$ there are three constellation points on the right half-plane of Figure 3-5 that must be considered:

Point 1 : $d_{k_2} + d_k = d_{k-1} + d_{k+1} = 0$ with probability 1/8

$$A_k = A_{k-1} = \sqrt{2P}C_G(0). \tag{A.70}$$

This is the case of ordinary DPSK with SNR equal to $A_k^2/2\sigma^2$. Using $E_B/N_0 = 2PT$ conditional BER is

$$BER(1) = \frac{1}{2} e^{-\frac{E_B}{N_0} \frac{\sqrt{2\pi} C_G^2(0)}{k_1 2BT}}. \tag{A.71}$$

Point 2 : $d_{k-2} + d_k = d_{k-1} + d_{k+1} = \pm 2$ with probability $1/8$

$$A_k = A_{k-1} = \sqrt{2P}(C_G + 2C_G(2T)) \tag{A.72}$$

and, similarly to the previous case

$$BER(2) = \frac{1}{2} e^{-\frac{E_B}{N_0} \frac{\sqrt{2\pi}}{k_1 2BT}(C_G(0)+2C_G(2T))^2}. \tag{A.73}$$

Point 3 : $d_{k-2} + d_k \neq d_{k-1} + d_{k+1}$ with probability $1/4$. Without loss of generality assume $d_{k-2} + d_k = \pm 2$ and $d_{k-1} + d_{k+1} = 0$, then

$$A_k = \sqrt{2P} C_G(0) \tag{A.74}$$

$$A_{k-1} = \sqrt{2P}(C_G(0) + 2C_G(2T)) \tag{A.75}$$

and

$$a_3 = \frac{E_B}{N_0} \frac{2\sqrt{2\pi}}{k_1 2BT} C_G^2(2T) \tag{A.76}$$

$$b_3 = \frac{E_B}{N_0} \frac{2\sqrt{2\pi}}{k_1 2BT}(C_G(0) + C_G(2T))^2. \tag{A.77}$$

$d_k \neq d_{k-1}$:

Because noise covariance is zero, Equation (A.69) is unchanged for this case.

Point 4 : $d_{k-2} + d_k = d_{k-1} + d_{k+1} = 0$ with probability $1/8$. This point reflects, and has the same BER, as point 1.

Point 5 : $d_{k-2} + d_k = d_{k-1} + d_{k+1} = \pm 2$ with probability $1/8$

$$A_k = \sqrt{2P}(C_G(0) - 2C_G(2T)) \tag{A.78}$$

$$A_{k-1} = \sqrt{2P}(C_G(0) - 2C_G(2T)) \tag{A.79}$$

and

$$BER(5) = \frac{1}{2} e^{-\frac{E_B}{N_0} \frac{\sqrt{2\pi}}{k_1 2BT}(C_G(0)-2C_G(2T))^2}. \tag{A.80}$$

Point 6 : $d_{k-2} + d_k \neq d_{k-1} + d_{k+1}$ with probability $1/4$. Without loss of generality, assume that $d_{k-2} + d_k = \pm 2$ and $d_{k-1} + d_{k+1} = 0$. Then

$$A_k = \sqrt{2P} C_G(0) \tag{A.81}$$

$$A_{k-1} = \sqrt{2P}(C_G(0) - 2C_G(2T)) \tag{A.82}$$

and

$$a_6 = \frac{E_B}{N_0} \frac{2\sqrt{2\pi}}{k_1 2BT} C_G^2(2T) \tag{A.83}$$

$$b_6 = \frac{E_B}{N_0} \frac{2\sqrt{2\pi}}{k_1 2BT} (C_G(0) - C_G(2T))^2. \tag{A.84}$$

Averaging over these six points results in the BER expression of Equation (3.17).

REFERENCES

1. R. DeBuda, "Coherent Demodulation of Frequency-Shift Keying with Low Deviation Ratio," *IEEE Trans. Commun.*, COM-20, 429–435 (1972).

2. L.S. Metzger, "Performance of Phase Comparison Sinusoidal Frequency Shift Keying," *IEEE Trans. Commun.*, COM-26, 1250–1253 (1974).

3. M.K. Simon and C.C. Wang, "Differential Detection of Gaussian MSK in a Mobile Radio Environment," *IEEE Trans. Veh. Technol.*, VT-33, 307–320 (1984).

4. M.K. Simon and C.C. Wang, "Two-Bit Differential Detection of MSK," *Procs. Global Communications Conf.*, 740–745 (1984).

5. G.K. Kaleh, "A Differentially Coherent Receiver for Minimum Shift Keying Signal," *IEEE J. Select. Areas Commun.*, 99–106 (1989).

6. M.K. Simon and C.C. Wang, "Differential Versus Limiter–Discriminator Detection of Narrow-Band FM," *IEEE Trans. Commun.*, COM-31, 1227–1234 (1983).

7. H.E. Salzer, "Formulas for Calculating the Error Function of a Complex Variable," *Math. Tables Other Aids Computation*, 67–70 (1951).

8. S. Stein, "Unified Analysis of Certain Coherent and Noncoherent Binary Communications Systems," *IEEE Trans. Inf. Theory*, IT-10, 43–51 (1964).

9. M. Schwartz, W.R. Bennet, and S. Stein, *Communication Systems and Techniques*, New York: McGraw-Hill, Chap. 8 (1966), pp. 314–342.

10. J.G. Proakis, *Digital Communications*, New York: McGraw-Hill (1983).

REPORT DOCUMENTATION PAGE

Form Approved
OMB No. 0704-0188

1. AGENCY USE ONLY *(Leave blank)*	2. REPORT DATE	3. REPORT TYPE AND DATES COVERED
	16 July 1990	Technical Report

4. TITLE AND SUBTITLE
Analysis of DMSK Demodulators for DMSK and DPSK Reception

5. FUNDING NUMBERS
C — F19628-90-C-0002
PE — 33110F, 33603F
PR — 370

6. AUTHOR(S)
Bruce F. McGuffin

7. PERFORMING ORGANIZATION NAME(S) AND ADDRESS(ES)
Lincoln Laboratory, MIT
P.O. Box 73
Lexington, MA 02173-9108

8. PERFORMING ORGANIZATION REPORT NUMBER
TR-883

9. SPONSORING/MONITORING AGENCY NAME(S) AND ADDRESS(ES)
HQ AF Space Systems Division SD/MH
Los Angeles AFB, CA 90009-2960

10. SPONSORING/MONITORING AGENCY REPORT NUMBER
ESD-TR-90-031

11. SUPPLEMENTARY NOTES
None

12a. DISTRIBUTION/AVAILABILITY STATEMENT
Approved for public release; distribution is unlimited.

12b. DISTRIBUTION CODE

13. ABSTRACT *(Maximum 200 words)*

This report considers some issues involved in using high data rate differential minimum shift keyed (DMSK) modulation to augment an existing satellite communication system employing differential phase shift keyed (DPSK) modulation. DMSK is preferred over DPSK for its greater spectral efficiency and robustness in nonlinear channels.

Two DMSK structures are discussed, the one- and two-bit demodulators, the second of which demodulates two interleaved differential data sequences. Analytic expressions are derived giving the bit error rate performance of both types of demodulator, with either matched or Gaussian filters. It is shown that the two-bit demodulator with a Gaussian filter provides the best performance in additive white Gaussian noise.

The use of a DMSK demodulator to receive DPSK signals is examined. This is of interest in order to reduce the number of demodulators required, while supporting augmented and original service. It is shown that the two-bit DMSK demodulator can be used to receive DPSK signals, but the one-bit demodulator cannot. Performance with filters that provide optimized DMSK demodulation and filters modified for DPSK signals are discussed. For a very small loss in DMSK performance, performance with DPSK signals can be brought to within 2 dB of the ideal DPSK demodulator.

14. SUBJECT TERMS		15. NUMBER OF PAGES
differential MSK differential PSK	DMSK/DPSK cross support	58
		16. PRICE CODE

17. SECURITY CLASSIFICATION OF REPORT	18. SECURITY CLASSIFICATION OF THIS PAGE	19. SECURITY CLASSIFICATION OF ABSTRACT	20. LIMITATION OF ABSTRACT
Unclassified	Unclassified	Unclassified	SAR